CZECH TECHNICAL UNIVERSITY IN PRAGUE

LULEÅ TEKNISKA UNIVERSITET

UNIVERSITY OF WEST BOHEMIA

spaCe master

Joint European Master in Space Science and Technology

DIPLOMA THESIS

Optical Attitude Determination Subsystem for PilsenCube PicoSatellite

By

Nagarjuna Rao Kandimala

May 2012

Optical Attitude Determination Subsystem for PilsenCube Pico Satellite

Nagarjuna Rao Kandimala

Submitted in partial fulfilment for the Degrees in

MSc with a Major in Space Technology

(Teknologie Masterexamen med huvudområde Rymdteknik)

from

Luleå University of Technology

and

MSc in Electrical Engineering and Informatics - Control Engineering

(MSc Elektrotechnika a informatika -Technicka kybernetika)

from

Czech Technical Univesity

May 2012

Author	**: Nagarjuna Rao Kandimala** **SpaceMaster Round-6**
Supervisor	**: Ing. Martin Hromcik, Ph.D.** **Czech Technical University** **Faculty of Electrical Engineering** **Department of Control Engineering** **Prague, The Czech Republic**
Supervisor	**: Dr.Anita Enmark** **Luleå University of Technology** **Department of Space Science** **Kiruna, Sweden**
Technical Supervisor	**: Ing. Ivo Vertat, Ph.D.** **University of West Bohemia** **Faculty of Electrical Engineering** **Department of Applied Electronics** **Pilsen, The Czech Republic**

Proclamation

I honestly claim that I have done my Diploma thesis all by myself and I have used only the materials (literature, projects, SW etc.) stated in the attached list.

In Prague,.....

Signature

Abstract

Today's Attitude Determination Subsystem (ADS) used by CubeSat class are expensive and complex to implement, this thesis is aimed at providing low cost, power efficient and simple to implement ADS solution for CubeSat class using Optical sensors. Three different optical sensors are used namely TPS-231, EPD-365 and BPW-21 for Infrared radiation, UV radiation and Visible radiation detection respectively. With these sensors arranged in the middle on all the walls 3-axis attitude determination is achieved. These sensors when irradiated by Sun or Earth or both, demonstrate different characteristics, which are used for estimating the attitude of the satellite by determining the position of Sun and Earth. Different relative positions of Sun and Earth are simulated and the simulation results were found to be satisfactory. An algorithm is proposed based on these simulations for low power ADCS computer. From the simulation results this solution demonstrates feasibility.

Contents

1 Introduction **1**
1.1 Brief History . . . 1
1.2 CubeSat Specifications . . . 1
1.3 Survey of CubeSat Attitude Determination Subsystem . . . 1
1.4 PilsenCube pico-Satellite ADS . . . 2

2 Optical Sensors Introduction **4**
2.1 Scientific Backgound . . . 4
2.1.1 Sun Irradiation AM0 . . . 5
2.1.2 Earth Albedo Radiation . . . 6
2.1.3 Earth Thermal Emission . . . 6
2.2 Technical Overview . . . 7
2.2.1 Photodiode . . . 7
2.2.2 Thermopile . . . 8
2.3 Sensors Specifications . . . 9
2.3.1 EPD-365 . . . 9
2.3.2 BPW-21 . . . 9
2.3.3 TPS-230 . . . 10

3 Calculations **10**
3.1 Ultraviolet sensor EPD-365 . . . 10
3.1.1 EPD-365 in Sun irradiation . . . 11
3.1.2 EPD-365 in Albedo irradiation . . . 12
3.2 Visible radiation sensor BPW-21 . . . 16
3.2.1 BPW-21 in Sun Irradiation . . . 16
3.2.2 BPW-21 in Albedo Irradiation . . . 18
3.3 Infrared Radiation sensor TPS-230 . . . 19
3.3.1 TPS-230 in Sun Thermal Radiation . . . 19
3.3.2 TPS-230 in Earth Thermal Emission . . . 19

4 Simulation Results **20**

5 Algorithm **22**

6 Conclusion **24**

7 Future work **24**

References **26**

A Appendix **27**
A.1 Matlab Code . . . 28
A.2 Datasheets . . . 38
A.2.1 EPD-365 Datasheet . . . 38
A.2.2 BPW-21 Datasheet . . . 41
A.2.3 TPS-230 Datasheet . . . 46
A.3 CD - Contents . . . 53

List of Figures

1 PilsenCube structure . . . 3
2 Functional Block Diagram of PilsenCube ADS . . . 4
3 Cross-section of the Sun [2] . . . 5
4 Electromagnetic Spectrum [9] . . . 5
5 Comparison of Spectral irradiation density [10] . . . 6
6 Linear plot of Spectral Irradiance from ASTM E-490 Data . . . 6
7 Log plot of Spectral Irradiance from ASTM E-490 Data . . . 7
8 Earth's Radiation Budget [6, page 241] . . . 7
9 Percentage Variation of Albedo with different surface conditions [7] . . . 8
10 Photodiode functional diagram . . . 8
11 Thermopile . . . 9
12 TPS-230 Sensor . . . 9
13 BPW-21 Sensor . . . 9
14 TPS-230 Sensor . . . 10
15 Relative Sensitivity for BWP-21 and EPD-365 . . . 11
16 $I_{P,Albedo}$ of EPD sensor . . . 16
17 $I_{P,Sun}$ of EPD sensor . . . 16
18 $I_{P,Albedo}$ of BPW sensor . . . 16
19 $I_{P,Sun}$ of BPW sensor . . . 16
20 Spectral Sensitivity for BWP-21 . . . 17
21 Ratio of TPS sensor . . . 20
22 Ratio of TPS sensor . . . 20
23 Output Voltage . . . 20
24 Sides of the CubeSat . . . 21
25 Ratio of TPS sensor . . . 21
26 Ratio of BPW sensor . . . 22
27 Ratio of BPW sensor . . . 22
28 Flow Chart . . . 25

List of Tables

1 CubeSat Specifications . . . 1
2 Survey of CubeSat ADCS . . . 2
3 Components used on PilsenCube . . . 3
4 EPD-365 specification . . . 9
5 BPW-21 specification . . . 10
6 TPS-230 specification . . . 10
7 $I_{totalNoise}$ of EDP-365 sensor . . . 13
8 $I_{totalNoise}$ of BPW-21 sensor . . . 13
9 I_P of EPD-365 sensor . . . 14
10 I_P of BPW-21 sensor . . . 14
13 SNR_{Sun} in db of BPW-21 sensor . . . 15
14 SNR_{Albedo} in db of BPW-21 sensor . . . 15
11 SNR_{Sun} in db of EPD-365 sensor . . . 15
12 SNR_{Albedo} in db of EPD-365 sensor . . . 15
15 SNR_{Albedo} in db of TPS-230 sensor . . . 20

Acknowledgements

It is with utmost respect and immense gratitude that I acknowledge the support of my supervisor, Dr. Ivo Vertat. He assisted me greatly during every phase of my research and work and I am thankful to him for helping me resolve problems with my work irrespective of his schedule and time.

I also take great pleasure to acknowledge my supervisor from the Czech Technical University, Dr. Martin Hromcik for accepting my thesis topic. Furthermore, I would like to thank my supervisor from the Luleå University of Technology, Dr. Anita Enmark and Dr. Johnny Ejemalm for supporting my thesis topic from the beginning. I would also like to acknowledge Czech Science Foundation, for supporting this thesis with registered projects number: 102/09/0455, under Power efficient space probe for experimental research based on Pico Satellite.

I would like to further extend my gratitude towards SpaceMaster consortium for crafting Spacemasters into Masters of the Space, honored to be a Spacemaster.

Last but not least, I give my profound gratitude to my parents for their support. Without them, I would not be where I am today.

-Nagarjuna Rao Kandimala

SpaceMaster Round-6

1 Introduction

1.1 Brief History

1957, dawn of the Space Age, with launch of the worlds first artificial satellite Sputnik-1 by the Soviet Union a new era of space have originated, after this many satellites with different mission have been launched most of them orbiting the Earth, some around the planets, some constantly monitoring the activity on the SUN and recent revolution of Voyager 1 and Voyager 2 satellites launched by NASA in 1977 is to cross the solar system. These satellites after flyby over different planets now are about to cross the heliopause. In these satellites the Attitude Determination Subsystem (ADS) execute a prominent role to maintain the pointing of the high gain antenna towards the Earth. Today the technology is leading us to miniaturizing, due to which a completely new class of satellites have emerged, they are Pico-satellites based on a new standard called CubeSats. Universities primarily develop these satellites, size of these satellites is in tens of centimeters, weighing between one to ten kilograms and usually cost in tens of thousands of Euros. As the CubeSats are becoming popular and their requirement for orientation is increasing, the ADS as become an important part of the design. For CubeSats high accuracy ADS is still in its infancy. This thesis will attempt to develop an ADS for this class of satellites using Optical sensors, benefitting the cost and weight factors.

1.2 CubeSat Specifications

In 1999, California Polytechnic University (Cal Poly), San luis Obispo and the Space Systems Development Laboratory (SSDL) at Stanford University collaborated to develop a standard for a pico-satellite design [1, p.1-9]. The aim was to develop and launch the satellites in most cost effective approach, with the focus on Universities and research institutes. As of now there are over 100 universities, high schools, private firms and government organizations that are developing CubeSats. This will facilitate groups to test new and innovative hardware (like Optical sensors for ADS, in PilsenCube) and software on actual satellites instead of relying on simulations. Due to its low weight the launch cost is low and in fact some organizations launch there country's University satellites for free. For example ISRO launches the University satellites in India for free, which reduces the cost even more. Now a student with sufficient funding and professional support can design, build, test and launch a satellite during his undergradutation or graduation period, which emphasizes on the development of future Space Engineers. The Table 1 shows the CubeSat standard specifications, only important parameters are listed for detailed specification refer[1].

Requirement	**Units**	**Quantity**
Stored Chemical Enegry	Watt-Hours	100
Total Mass Loss(TML)	%	$\leq$1
Collected Volatile Condensable Material (CVCM)	%	$\leq$0.1
X and Y dimensions(width)	mm	100.0$\pm$0.1
Z dimension(height) (1U)	mm	113.5$\pm$0.1
Z dimension(height) (3U)	mm	340.5$\pm$0.3
Minimum Rails width	mm	8.5
Mass (1U)	kg	$\leq$ 1.33
Mass (3U)	kg	$\leq$4.0
Center of gravity from geometric center	cm	2

Table 1: CubeSat Specifications

1.3 Survey of CubeSat Attitude Determination Subsystem

Table 2 shows the CubeSat mission that have been launched, the list is not a complete list, but covers all kinds of attitude sensors used so far. The missions so far flown are low in accuracy as the high accuracy

ADS is complex and expensive. Star tracker being the high accurate sensor is not flown yet as it is very expensive for university budget.

Apart from this there are some pre-packed ADS available in the market like the Pumpkin IMI-100 ADADS and SFL ADCS, which satisfies the CubeSate Standard and provide accuracy of about 1 degree.

Organization	**CubeSat**	**Launch**	**ADS**
Tokyo Institute of Technology	CUTE-I	2003	MEMS Gyro, 2 Axis Accelerometer, Sun sensor
University of Tokyo	XI-IV	2003	Permanent Magnet and hysteresis rod
University of Toronto	CanX-1	2003	Horizon Sensor and Star tracker, Magnetometer, GPS
Technical University of Denmark	DTUsat	2003	MEMS Sun Sensor, Magnetometer
Alborg University	AAU Cubesat	2003	Sun Sensor, Magnetometer
Stanford University and Quakesat LLC	Quake Sat	2003	Magnetometer
Norwegian U of Science and Technology	NCube2	2005	Magnetometer
University of Wurzburg	UWE-1	2005	N/A
University of Tokyo	XI-V	2005	Camera
Tokyo Institute of Technology	CUTE 1.7 + APD	2006	Gyro, Magnetometer, Sun Sensor, Earth Sensor
University of Kansas	KUTEsat Pathfinder	2006	Magnetometer, Sun Sensor
California Polytechnic Institute	CP2	2006	Magnetometer
California Polytechnic Institute	CP1	2006	Sun Sensor
The Boeing Comapny	CSTB-1	2007	Sun Sensor, Magnetometer
University of Sergio Arboleda	Libertad-1	2007	GPS receiver
Delft University of Technology	Delfi-C3	2008	Sun Sensor
Alborg Univesity	AAUsat-2	2008	Magnetic Coils, Momentum Wheel
Fachhochschule Aachen	Compass One	2008	Magnetometer, Sun Sensor, Magnetorquers
California Polytechnic State University	Polysat CP6	2009	Magnetometer
University of Trieste	AtmoCube	2010	Magnetometer, GPS receiver
University of Bucharest	Goliat	2010	Magnetometer, GPS receiver, 2 Axes Momentum Wheel
Warsaw University of Technology	PW-Sat	2010	Magnetometer, MEMS gyroscope, GPS receiver, Magnetorquers
Polytechnical School of Lausanne	SwissCube	2010	Sun Sensor, Magnetometer, gyro, Magnetorquers
University of Wuerzburg	UWE-3	2010	N/A
SRM University	SRMSAT	2011	Magnetometer, GPS, Magnetotorquers
Indian Institute of Technology	Jugnu	2011	MEMS based IMU, GPS

Table 2: Survey of CubeSat ADCS

1.4 PilsenCube pico-Satellite ADS

Unlike the traditional sensors like Sun sensor for Sun position determination and horizon sensor for Earth position determination, PilsenCube is implementing cost and power efficient technique for attitude determination using optical sensors, as per the survey conducted by the author the use of Optical sensors

Component	Model	Quantity	Purpose
Infrared Sensor	TPS-230	6	To measure thermal emission of Earth
Visible Sensor	BPW-21	6	To measure Sun irradiation and Earth backscattered radiation
Ultraviolet Sensor	EPD-365	6	To measure Sun irradiation and Earth backscattered UV radiation
MEMS 2-axis Gyroscope	LPR-530	1	To measure angular rate along pitch and roll axes
MEMS 1-axis Gyroscope	LY530	1	To measure angular rate along yaw axes
3-axis Magnetometer	HMC5883	1	To measure the strength and direction of magnetic field
FM broadcasting RDS receiver	AR-1000	1	To receive time and country code when the satellite wakesup from no supply

Table 3: Components used on PilsenCube

is first of its kind for CubeSat as per the survey table 2 . On successful implementation and testing of this experimental ADS on PilsenCube Pico satellite, this can be the cheapest solution with acceptable accuracy for CubeSat class. Table 3 gives the details about the key components used in PilsenCube.
Figure 2 shows the basic functional block diagram of the PilsenCube Pico satellite ADCS. Using TLE the initial satellite location is determined and in case of satellite wake up from temporary power failure, the existing two line element information cannot be used in this case RDS signal from FM broadcasting it will receive time and country code for position determination, this data will be used by main computer for the radio beacon transmission control and for triggering the antenna to orient towards the home ground station. The optical sensors are used for satellite orientation to determine which wall is pointing towards Sun, Earth and free space, using this data antenna can be oriented towards Earth and solar panels can be oriented towards Sun. The main computer for planning the radio transmission and attitude control switching can use this data. The Pico satellite rotation measurement block gives angular rate measurement of Yaw, Pitch and Roll angles. All the data is used by ADCS computer which signals the three orthogonal wired magnetic coils and acquires the required attitude control.

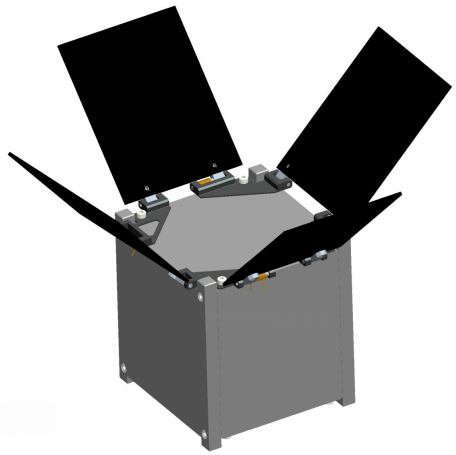

Figure 1: PilsenCube structure

Figure 1 shows the satellite structure, all the wall are equipped with the optical sensors, almost in the center. The main objective of this work is to compute the output signal from the optical sensors (TPS-230, EPD-365 and BPW-21) in all angles and directions with respect to Earth and Sun, simulate the sensors output during Pico satellite rotation with several relative positions of Earth and Sun, finally, implementing an algorithm to estimate the position of Sun and Earth in satellite reference frame.

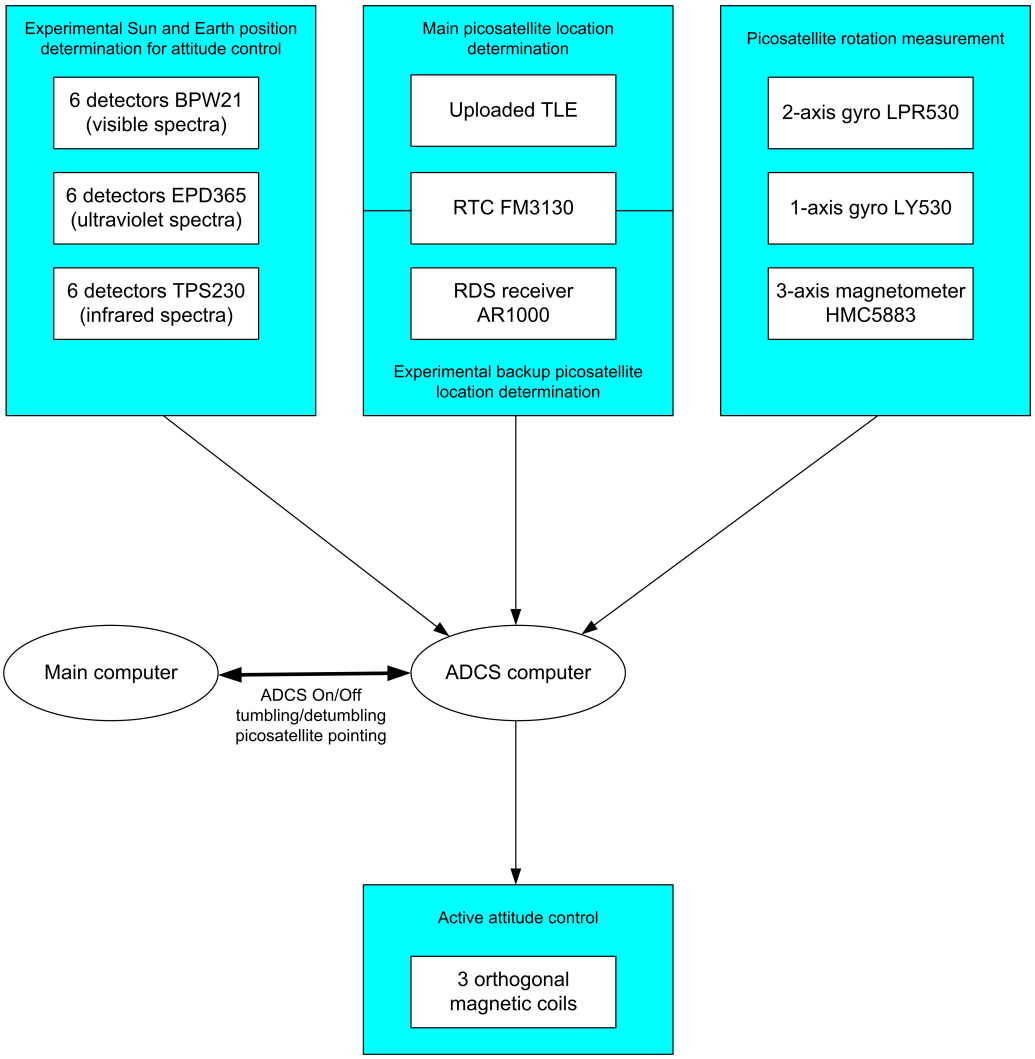

Figure 2: Functional Block Diagram of PilsenCube ADS

2 Optical Sensors Introduction

In this section a scientific background associated to the sensors is focused briefly followed by the technical description of the sensors and sensors specifications.

2.1 Scientific Backgound

Sun is the main source of energy for the solar system, delivering energy to the Earth in the form of electro magnetic radiation.The spectrum of this electro magnetic radiation covers wide range of wavelengths from 0.0 to 14000nm[8]. Figure 3 shows the cross-section of the Sun, seen are the different radiation tags, temperature at core and at surface, sunspots and coronal loops etc. Figure 4 shows the different

wavelengths and there intensity. For this thesis UV radiation with wavelengths from 240nm to 400nm, Visible radiation from 400nm to 700nm and Infrared radiation from 7500 to 13500nm are of interest. In this sub-section a brief description about the Sun irradiation AM0, Earth Albedo radiation and Earth thermal emission are comprehended.

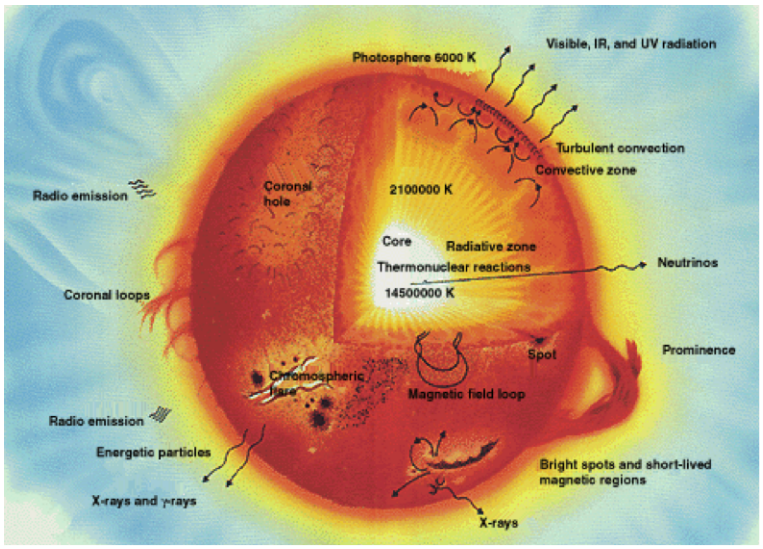

Figure 3: Cross-section of the Sun [2]

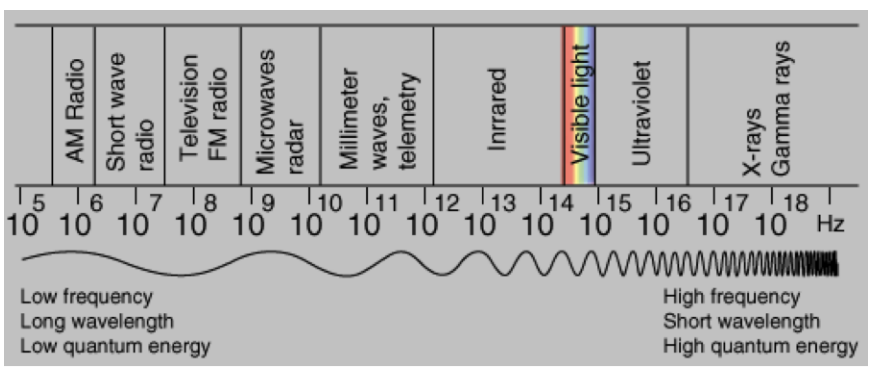

Figure 4: Electromagnetic Spectrum [9]

2.1.1 Sun Irradiation AM0

Air Mass (AM) is the reduction in the intensity of sunlight due to the absorption in the Earths atmosphere, usually by air and dust. In Earth orbit this value is 0 due to the absence of atmosphere, so the name AM0. The Air Mass is different for different locations on the Earth, for example, Central Europe and North America as AM1.5 where as at equator it is AM1. Figure 5 shows the difference between the Spectral irradiation density of Blackbody (Sun at 6000K), AM0 (Earth orbit) and AM1.5. This thesis is limited to sun irradiation AM0.

On observing the Figure 5 the UV light as a significant decrease between AM0 and AM1.5, this is due to the absorption of UV by the Ozone layer of the upper atmosphere. This phenomenon can be used by the Sensors onboard of PilsenCube to determine the direction of Sun and Earth.

For the simulation of the sensors in sun irradiation AM0, data from ASTM-E-490 is used [13]. This data is ideal for the optical sensor power density calculations. The plots from this data are shown in figure 6 and figure 7 covering the spectrum of interest from about 240nm to 13500nm.

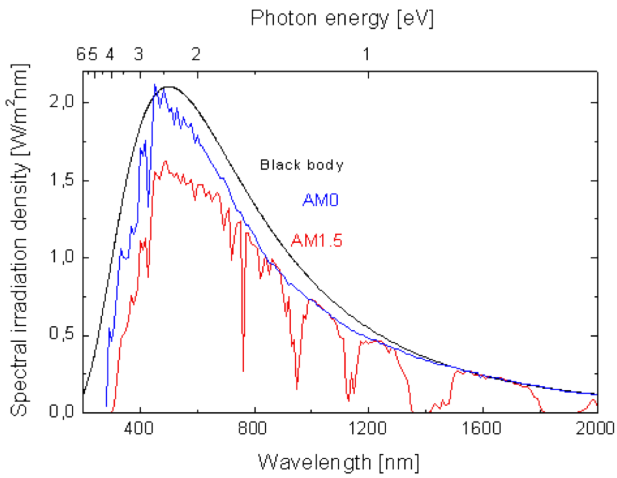

Figure 5: Comparison of Spectral irradiation density [10]

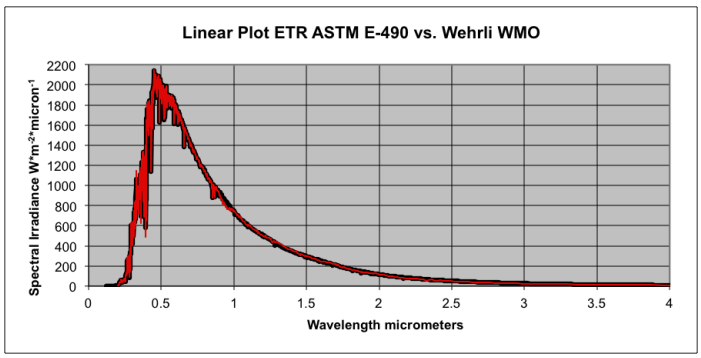

Figure 6: Linear plot of Spectral Irradiance from ASTM E-490 Data

2.1.2 Earth Albedo Radiation

Albedo of the Earth can be defined as the total amount of solar radiation reflected back to the Space, due to different surfaces, vegetation, ocean, snow, aerosols etc. The average Albedo of Earth is estimated to be 30% of total solar radiation incident on Earth in visible range of wavelength, for the UV range of wavelengths it is smaller probably due to the absorption in ozone layer. Figure 8 shows the solar energy that dispersed on the Earth and radiated back to the space. The shown values are in $PW = 10^{15}$ Watt. Figure 9 shows the percentages of reflection by different surfaces.

For the simulation of the sensors in Earth albedo radiation, data from ASTM-E-490 is used in visible range by taking 30% of the total power density, and for UV range data from SSBUV [14] is used, but the in SSBUV data UV reflectivity is calculated as a mean value over 12 ultraviolet wavelengths at different longitude and latitude, so to validate this data for the calculation of Power density, mean value of reflectivity over all latitude and longitude is considered and this obtained value is multiplied with the ASTM-E-490 data. This way approximate power density of albedo in UV wavelength is obtained.

2.1.3 Earth Thermal Emission

The thermal radiation from Sun can be referred as short wave radiation and the Earths thermal radiation can be referred as long wave radiation. The radiation from Earth has lower intensity and different spectral distribution, as it is cooler. The incoming solar radiation (shortwave) and outgoing energy (long wave) from the Earth governs surface temperature and the greenhouse effect. At thermal equilibrium, the

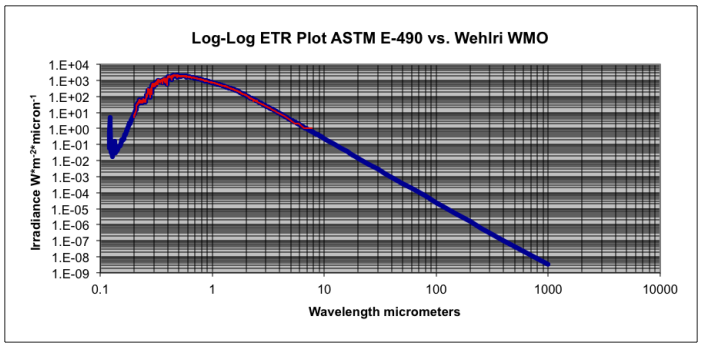

Figure 7: Log plot of Spectral Irradiance from ASTM E-490 Data

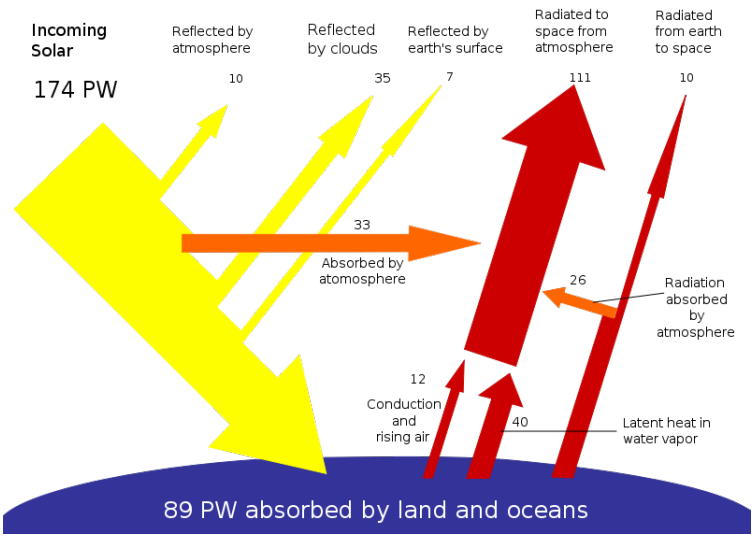

Figure 8: Earth's Radiation Budget [6, page 241]

emissivity of the body equals its absorptivity as proposed by Gustav Kirchhoff in 1859, which suggests that the Earth can be approximated to a Blackbody. The temperature of the Earth (or any planet orbiting Sun) can be determined by the Blackbody law, which depends on several factors like shortwave radiation, long wave radiation, Albedo etc.
Energy emitted from the Earth and atmosphere into space (related to their physical temperature) is the Earth Thermal Emission, this emission is detectable both on day and in Earths shadow. Earths ambient temperature is about 300°K and radiates 160,000 times less than the sun and whole energy is radiated at thermal infrared wavelengths between 4-25µm with maximum emission at about 9.7µm [11].

2.2 Technical Overview

The Optical sensors in the PilsenCube fall into two categories, namely Photodiode and Thermopile. EPD-365 (UV sensor) and BPW-21 (Visible light sensor) are photodiodes and TPS-230 (Infrared sensor) is a thermopile sensor. In this sub-section working principles of the sensors is provided.

2.2.1 Photodiode

These types of photo sensors convert the light into current (in our case) or voltage based on the mode of operation. In zero bias or photovoltaic mode, photocurrent is restricted due to which voltage builds up. In reverse bias or photoconductive mode the photocurrent is produced and also response time is faster

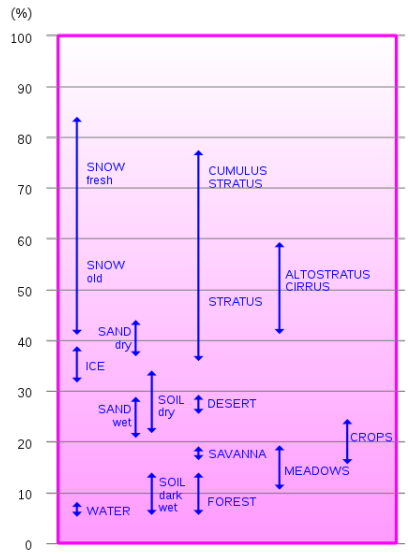

Figure 9: Percentage Variation of Albedo with different surface conditions [7]

due to decrease in the junction capacitance. Figure 10 shows the cross section of the photodiode.

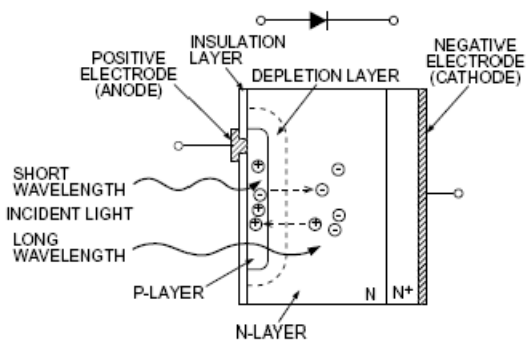

Figure 10: Photodiode functional diagram

Principle of operation

Photodiodes are based on p-n junction or PIN structure. When a sufficient energy Photon hits the diode, it excites an electron, which will create a free electron and positively charged electron hole. When the absorption occurs in the depletion junction the field of the depletion region sweeps the carriers. Thus holes move towards Anode and electrons move towards Cathode, due to this process Photocurrent is generated. The generated photocurrent is the sum of both the dark current and the light current, so the dark current must be minimized to enhance the sensitivity[12].

2.2.2 Thermopile

Thermopiles are made from a set of thermocouple junctions, which are connected electrically in series. Thermopiles convert the incoming radiation to voltage. This effect is known as thermoelectric or Seebeck coefficient.

Principle of operation

The operational principle is similar to that of the thermocouple, as the voltage of a single thermocouple is very low; lots of such thermocouples are connected in series to obtain high voltages. In TPS-230 sensor a special IR absorption layer covers the hot junctions creating the sensors active area. When this sensor is exposed to the infrared radiation, the energy absorbed leads to temperature difference between the hot and cold contacts, which is thermoelectric coefficient and a voltage is generated.

Figure 11: Thermopile

2.3 Sensors Specifications

In this section the sensors specifications are provided. The specifications of the sensors are tabulated in the respective sub sections and for further reference datasheets are provided in the Appendix A.2.

2.3.1 EPD-365

This sensor has wide bandwidth and high spectral sensitivity in the UV range (245nm 400nm) with Schottky type contact using GaP technology and mounted in hermetically sealed TO-46 package with UG11 UV filter-glass window. Figure 12 shows the sensor and Table 4 provides the specification of the sensor. For detailed specification refer A.2.1.

Figure 12: TPS-230 Sensor

Parameter	Test Condition	Value	Unit
Wavelength range	-	245 to 400	nm
Active Area	-	1.2	mm^2
Temperature coefficient of Dark current	-	7.0	$\%/K$
Operating temperature range	-	-40 to +125	$^\circ C$
Dark current	$T_{amb} = 25^\circ C, V_R = 5V$	5	pA
Responsivity at $365nm$	$V_R = 0V$	0.07	A/W
Shunt resistance	$V_R = 10mV$	150 to 200	$G\Omega$
Noise Equivalent Power at $365nm$	$V_R = 5V$	$1.8*10^{-14}$	$W/\sqrt{Hz}$

Table 4: EPD-365 specification

2.3.2 BPW-21

This sensor has wide bandwidth in Visible range (350nm-820nm) and is mounted in hermetically sealed TO-5 metal package. Figure 13 shows the sensor and Table 5 provides the specification of the sensor. For detailed specification refer A.2.2.

Figure 13: BPW-21 Sensor

Parameter	Test Condition	Value	Unit
Wavelength range	-	350 to 820	nm
Active Area	-	7.34	mm^2
Temperature coefficient	-	-0.05	$\%/K$
Operating temperature range	-	-40 to +80	$^\circ C$
Dark current	$T_{amb} = 25^\circ C, V_R = 10mV$	8	pA
Responsivity at $550nm$	$T_{amb} = 25^\circ C$	0.34	A/W
Shunt resistance	$V_o = 400mV$	39.769	$K\Omega$
Noise Equivalent Power at $550nm$	$V_R = 5V$	$7.2*10^{-14}$	$W/\sqrt{Hz}$

Table 5: BPW-21 specification

2.3.3 TPS-230

This sensor is based on thermopile sensing principle, which allows for broadband IR measurement and is mounted in TO-41 metal cap with integrated IR window and insulation gas sealing for leak proof of the dry nitrogen inside the sensor. Figure 14 shows the sensor and Table 6 provides the specification of the sensor. For detailed specification refer A.2.3.

Figure 14: TPS-230 Sensor

Parameter	Test Condition	Value	Unit
Wavelength range	-	750 to 1350	nm
Active Area	-	0.2	mm^2
Temperature coefficient of sensitivity	-	-0.05	$\%/K$
Temperature coefficient of resistance	-	0.03	$\%/K$
Operating temperature range	-	-20 to +100	$^\circ C$
Responsivity	$T_{amb} = 25^\circ C, Tobj = 227^\circ C$	42	V/W
Resistance	-	6.5 to 968.201	$K\Omega$
Noise voltage	-	40	$nV/\sqrt{Hz}$

Table 6: TPS-230 specification

3 Calculations

In this section the output signals from the Optical sensors in all angles and direction against the Earth (TPS sensor) and Sun (BPW and EPD sensors) from LEO are calculated and plotted.

3.1 Ultraviolet sensor EPD-365

EPD-365 sensor is used to monitor the UV radiation from Sun and Earth, providing further accuracy to the Visible sensor, as the satellite wall pointing towards Sun will have high temperatures due to which Infrared sensor may generate high output noise. UV sensor has lower sensitivity towards the temperature, due to which this sensor contributes to the accuracy to Sun position determination. For indemnity the wavelength used is 240nm to 410nm. Calculations of EPD-365 are shown in sections 3.1.1 and 3.1.2 and are tabulated in Tables 9, 7, 11 and 12.

3.1.1 EPD-365 in Sun irradiation

In this section output signals of EPD-365 in Sun irradiance are calculated. Only a sample calculation is provided, with 0° to 90° irradiance angle are tabulated. figure 17 details all the angles against Sun irradiance.

$$I_{p,SUN}(\varphi) = S_{rel}(\varphi) * ActiveArea * \sum_{i=1}^{n}(PowerDensity(\lambda_i) * SpectralSensitivity(\lambda_i) * \Delta\lambda) \quad (1)$$

Where,
$\Delta\lambda = \lambda_{i+1} - \lambda i$
$Active\ area\ of\ sensor = 1.2 * 10^{-6} m^2$

$$\sum_{i=1}^{n}(PowerDensity(\lambda_i) * SpectralSensitivity(\lambda_i) * \Delta\lambda) = 5.15\ [A/m^2]$$

This value is calculated from the Sun irradiance AM0 ASTM-E-490 data. This data can be downloaded from [13]. Value from the file (in $[W/m^2]$) is multiplied with the active area of the sensor to obtain the power of light at the input of sensor, this value is then converted into current (in case of BPW & EPD) by multiplying sensitivity value (A/W) of the sensor, which is the function of wavelength and angle of irradiance to obtain the photocurrent as a function of angle of irradiance, as shown by equation 1. S_{rel} depends on the angle of irradiance, shown in figure 15, different S_{rel} values at different angles possible are tabulated in Table 9.

$Let\ us\ consider \varphi = 0°$

$$I_{p,SUN}(0) = 1 * 1.2 * 10^{-6} m^2 * 5.15 = 6.18 * 10^{-6}\ [A]$$

$Considering\ the\ temperature\ of\ sensor = 50°$
$Given\ Temperatrue\ Coefficient = 7\%/K$

$$I_d(50°C) \ = 5 * 10^{-12} * 1.07^{(50°C - 25°C)} = 4 * 10^{-10}\ [A]$$

This method is considered over using the NEP parameter from the data sheet, as the NEP value needs correction for different temperatures, so this method is considered to be appropriate.

$$I_{totalnoise} = \sqrt{I_S^2 + I_T^2} \quad (2)$$

where,

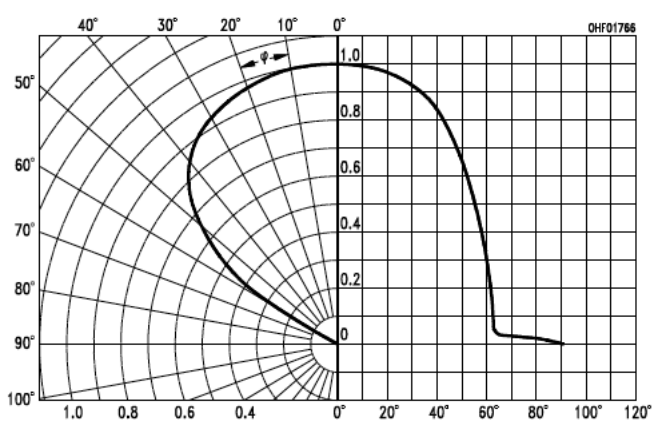

Figure 15: Relative Sensitivity for BWP-21 and EPD-365

$$
\begin{aligned}
ShotNoiseI_S &= \sqrt{2 * q * I_d * B} \\
&= \sqrt{2 * 1.6 * 10^{-19} * 4 * 10^{-10} * 10} \\
&= 3.577 * 10^{-14}\ [A] \\
ThermalNoiseI_T &= \sqrt{\frac{4 * k_b * T * B}{R_{SH}}} \\
&= \sqrt{\frac{4 * 1.38 * 10^{-23} * 323 * 10}{2 * 10^{11}}} \\
&= 1.00093 * 10^{-15}\ [A] \\
\therefore I_{totalnoise} &= 3.5791 * 10^{-14}\ [A] \\
SNR_{db} &= 20 * Log\left(\frac{I_p}{I_{totalnoise}}\right) \\
&= 20 * Log\left(\frac{6.18 * 10^{-6}}{3.5791 * 10^{-14}}\right) \\
&= 165db
\end{aligned}
$$

All the calculated Photocurrents as a function of irradiation angle are tabulated in Table 9.
As the Dark Current I_D depends on temperature of the sensor and contributing to the total noise current, the I_D and $I_{totalNoise}$ are computed at different temperatures and are tabulated in Table 7. The SNR values are computed and tabulated in Table 11. Here at angle 0° the SNR is computed for different possible temperatures.

3.1.2 EPD-365 in Albedo irradiation

Now photocurrent with respect to Albedo are calculated, as the sensor view the Earth disc at greater angle approximately 130° from 700km orbit, it is appropriate to consider the mean value of relative sensitivity over the angle range of Earth disc. In the equation 3 the value 0.2290 is the mean value of the reflectivity from SSBUV data. This data can be downloaded from [14, year-1996]. This data gives the UV reflectivity as a function of latitude and longitude, to obtain the power density of the Albedo, mean value of UV reflectivity over all latitude and longitude is considered, which is then multiplied by the power density data from Sun AM0 data. This approach is considered due to unavailability of data for UV reflectivity as a function of wavelength. Using this power density value photocurrents are calculated in equation 3.In this section output signals of EPD-365 in Earth backscattered UV radiation are calculated. Only a sample calculation is provided, with 0° to 90° irradiance angle tabulated. figure 16 details all the angles against Backscattered UV radiation.

$$
I_{p,Albedo}(\varphi) = S_{mean}(\varphi) * ActiveArea * \sum_{i=1}^{n}(0.2290 * PowerDensity(\lambda_i) * SpectralSensitivity(\lambda_i) * \Delta\lambda) \tag{3}
$$

$$
\sum_{i=1}^{n}(0.2290 * PowerDensity(\lambda_i) * SpectralSensitivity(\lambda_i) * \Delta\lambda) = 1.1797\ [A/m^2]
$$

S_{mean} depends on the angle of irradiation and Earth disc and the value, the figure 15 shows the relative sensitivity of the sensor, different S_{mean} values at different angles possible are tabulated in Table 9 and it has no units as it represents mean value of relative directional sensitivity over the Earth disc in the filed of view.

Let us consider $\varphi = 0°$

$$S_{mean}(0) = \frac{(1_{(0^\circ)} + 2 * 0.995_{(\pm 5^\circ)} + 2 * 0.99_{(\pm 10^\circ)} + 2 * 0.98_{(\pm 15^\circ)} + ...)}{27} = 0.76$$

$$I_{p,Albedo}(0) = 0.76 * 1.2 * 10^{-6} m^2 * 1.1797 = 1.08 * 10^{-6}\ [A]$$

$Considering\ the\ temperature\ of\ sensor = 50^\circ C$
$Given\ Temperatrue\ Coefficient = 7\%/K$

$$I_d(50^\circ C)\ = 5 * 10^{-12} * 1.07^{(50^\circ C - 25^\circ C)} = 4 * 10^{-10}\ [A]$$

Consider equation 2, to calculate the total noise current.

$$\begin{aligned}
ShotNoiseI_S &= \sqrt{2 * q * I_d * B} \\
&= \sqrt{2 * 1.6 * 10^{-19} * 4 * 10^{-10} * 10} \\
&= 3.577 * 10^{-14}\ [A] \\
Thermal\ Noise\ I_T &= \sqrt{\frac{4 * k_b * T * B}{R_{SH}}} \\
&= \sqrt{\frac{4 * 1.38 * 10^{-23} * 323 * 10}{2 * 10^{11}}} \\
&= 1.00093 * 10^{-15}\ [A] \\
\therefore I_{totalnoise} &= 3.5791 * 10^{-14} \\
SNR_{db} &= 20 * Log\left(\frac{I_p}{I_{totalnoise}}\right) \\
&= 20 * Log\left(\frac{1.08 * 10^{-6}}{3.5791 * 10^{-14}}\right) \\
&= 150db
\end{aligned}$$

Temp [$^\circ C$]	**Dark Current,** I_D [A]	**Shot Current,** I_S [A]	**Thermal Noise,** I_T[A]	**Total Noise Current,** $I_{totalNoise}$ [A]
25	5.00E-12	4.00E-15	9.07E-16	4.10E-15
50	4.00E-10	3.58E-14	9.44E-16	3.58E-14
75	4.00E-10	3.58E-14	9.80E-16	3.58E-14
100	4.00E-10	3.58E-14	1.01E-15	3.58E-14

Table 7: $I_{totalNoise}$ of EDP-365 sensor

Temp [$^\circ C$]	**Dark Current,** I_D [A]	**Shot Current,** I_S [A]	**Thermal Noise,** I_T[A]	**Total Noise Current,** $I_{totalNoise}$ [A]
25	8.00E-12	5.06E-15	2.03E-12	2.03E-12
50	8.00E-12	5.06E-15	2.11E-12	2.11E-12
75	8.00E-12	5.06E-15	2.19E-12	2.19E-12
100	8.00E-12	5.06E-15	2.27E-12	2.27E-12

Table 8: $I_{totalNoise}$ of BPW-21 sensor

Angle of Irradiance [deg]	**Relative Sensitivity** S_{rel}	**Photocurrent** $I_{P,Sun}$ [A]	**Mean Sensitivity** S_{mean}	**Photocurrent** $I_{P,Albedo}$ [A]
0	1.000	6.18E-06	0.760	1.08E-06
5	0.996	6.16E-06	0.760	1.08E-06
10	0.986	6.10E-06	0.754	1.07E-06
15	0.970	6.00E-06	0.739	1.05E-06
20	0.950	5.87E-06	0.715	1.01E-06
25	0.888	5.49E-06	0.685	9.70E-07
30	0.770	4.76E-06	0.652	9.23E-07
35	0.629	3.89E-06	0.617	8.74E-07
40	0.500	3.09E-06	0.582	8.24E-07
45	0.370	2.29E-06	0.550	7.79E-07
50	0.229	1.42E-06	0.517	7.33E-07
55	0.111	6.84E-07	0.481	6.82E-07
60	0.050	3.09E-07	0.443	6.27E-07
65	0.032	1.99E-07	0.403	5.71E-07
70	0.019	1.19E-07	0.363	5.14E-07
75	0.010	6.40E-08	0.324	4.59E-07
80	0.005	3.09E-08	0.286	4.05E-07
85	0.002	9.55E-09	0.251	3.56E-07
90	0.000	0.00E+00	0.220	3.11E-07

Table 9: I_P of EPD-365 sensor

Angle of Irradiance [deg]	**Relative Sensitivity** S_{rel}	**Photocurrent** $I_{P,Sun}$ [A]	**Mean Sensitivity** S_{mean}	**Photocurrent** $I_{P,Albedo}$ [A]
0	1.000	1.17E-03	0.760	2.66E-04
5	0.996	1.16E-03	0.760	2.66E-04
10	0.986	1.15E-03	0.754	2.64E-04
15	0.970	1.13E-03	0.739	2.58E-04
20	0.950	1.11E-03	0.715	2.50E-04
25	0.888	1.04E-03	0.685	2.40E-04
30	0.770	8.98E-04	0.652	2.28E-04
35	0.629	7.34E-04	0.617	2.16E-04
40	0.500	5.83E-04	0.582	2.04E-04
45	0.370	4.32E-04	0.550	1.92E-04
50	0.229	2.67E-04	0.517	1.81E-04
55	0.111	1.29E-04	0.481	1.69E-04
60	0.050	5.83E-05	0.443	1.55E-04
65	0.032	3.75E-05	0.403	1.41E-04
70	0.019	2.24E-05	0.363	1.27E-04
75	0.010	1.21E-05	0.324	1.13E-04
80	0.005	5.83E-06	0.286	1.00E-04
85	0.002	1.80E-06	0.251	8.79E-05
90	0.000	0.00E+00	0.220	7.70E-05

Table 10: I_P of BPW-21 sensor

SNR [db]	**25°C**	**50°C**	**75°C**	**100°C**
0	175	175	175	174
5	175	175	174	174
10	175	175	174	174
15	175	175	174	174
20	175	174	174	174
25	174	174	173	173
30	173	173	172	172
35	171	171	171	170
40	169	169	169	168
45	167	166	166	166
50	162	162	162	161
55	156	156	155	155
60	149	149	149	148
65	145	145	145	144
70	141	141	140	140
75	135	135	135	135
80	129	129	129	128
85	119	119	118	118
90	-Inf	-Inf	-Inf	-Inf

Table 13: SNR_{Sun} in db of BPW-21 sensor

SNR [db]	**25°C**	**50°C**	**75°C**	**100°C**
0	162	162	162	161
5	162	162	162	161
10	162	162	162	161
15	162	162	161	161
20	162	161	161	161
25	161	161	161	160
30	161	161	160	160
35	161	160	160	160
40	160	160	159	159
45	160	159	159	159
50	159	159	158	158
55	158	158	158	157
60	158	157	157	157
65	157	157	156	156
70	156	156	155	155
75	155	155	154	154
80	154	154	153	153
85	153	152	152	152
90	152	151	151	151

Table 14: SNR_{Albedo} in db of BPW-21 sensor

SNR [db]	**25°C**	**50°C**	**75°C**	**100°C**
0	184	165	165	165
5	184	165	165	165
10	183	165	165	165
15	183	164	164	164
20	183	164	164	164
25	183	164	164	164
30	181	162	162	162
35	180	161	161	161
40	178	159	159	159
45	175	156	156	156
50	171	152	152	152
55	164	146	146	146
60	158	139	139	139
65	154	135	135	135
70	149	130	130	130
75	144	125	125	125
80	138	119	119	119
85	127	109	109	109
90	-Inf	-Inf	-Inf	-Inf

Table 11: SNR_{Sun} in db of EPD-365 sensor

SNR [db]	**25°C**	**50°C**	**75°C**	**100°C**
0	168	150	150	150
5	168	150	150	150
10	168	149	149	149
15	168	149	149	149
20	168	149	149	149
25	167	149	149	149
30	167	148	148	148
35	167	148	148	148
40	166	147	147	147
45	166	147	147	147
50	165	146	146	146
55	164	146	146	146
60	164	145	145	145
65	163	144	144	144
70	162	143	143	143
75	161	142	142	142
80	160	141	141	141
85	159	140	140	140
90	158	139	139	139

Table 12: SNR_{Albedo} in db of EPD-365 sensor

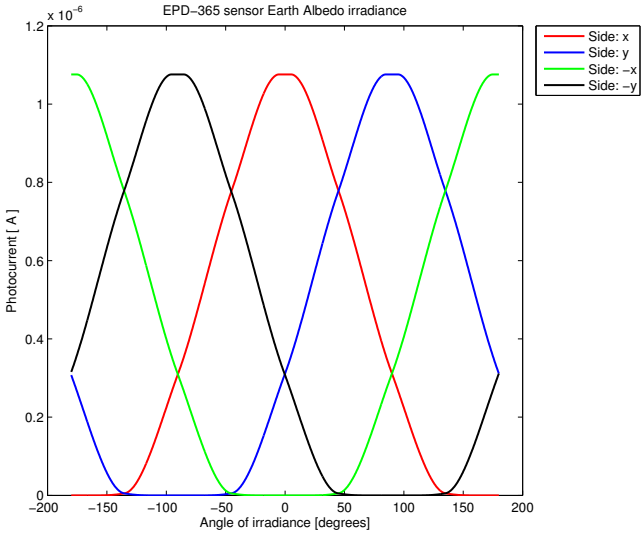

Figure 16: $I_{P,Albedo}$ of EPD sensor

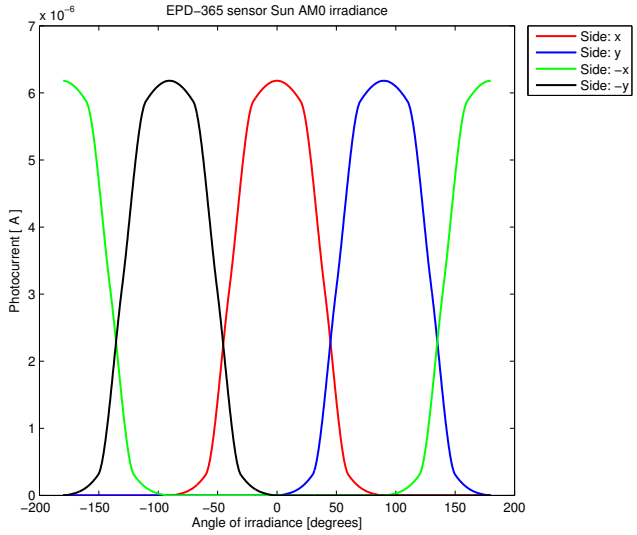

Figure 17: $I_{P,Sun}$ of EPD sensor

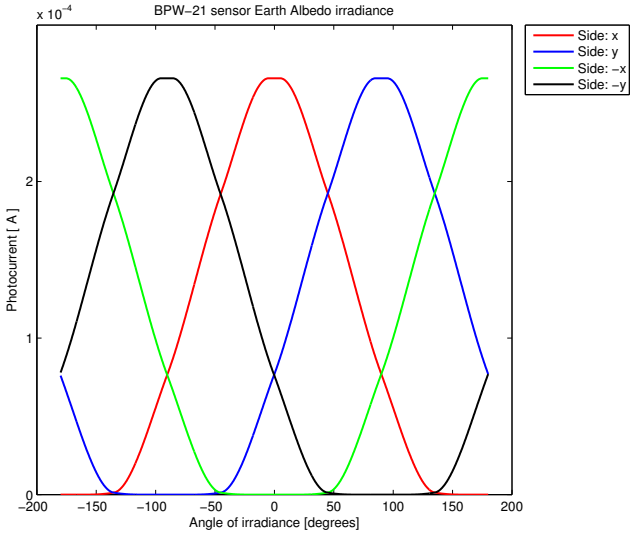

Figure 18: $I_{P,Albedo}$ of BPW sensor

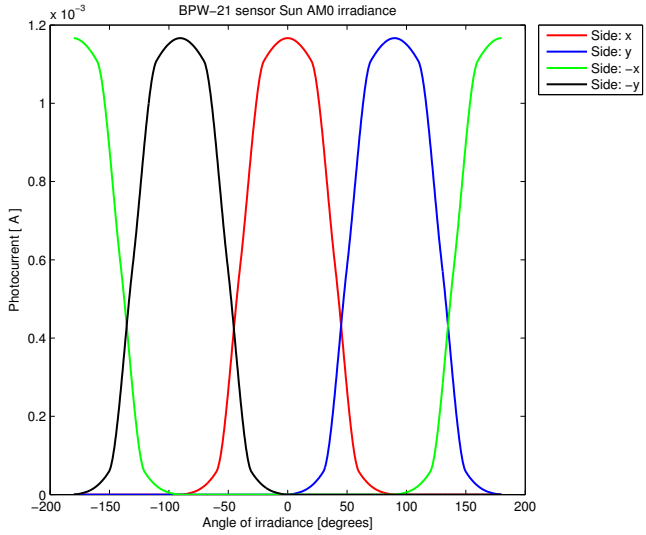

Figure 19: $I_{P,Sun}$ of BPW sensor

3.2 Visible radiation sensor BPW-21

This sensor is used to monitor the visible radiation from Sun and Earth. During the day period this sensor will be prominent sensor along with the EPD-365. For indemnity the wavelength used is 350nm to 1100nm. Calculations of BPW-21 are shown in sections 3.2.1 and 3.2.2 and are tabulated in the Tables 10, 8, 13 and 14.

3.2.1 BPW-21 in Sun Irradiation

In this section output signals of BPW-21 in Sun irradiance are calculated. Only a sample calculation is provided, with 0° to 90° irradiance angle are tabulated. Figure 19 details all the angles with respect to

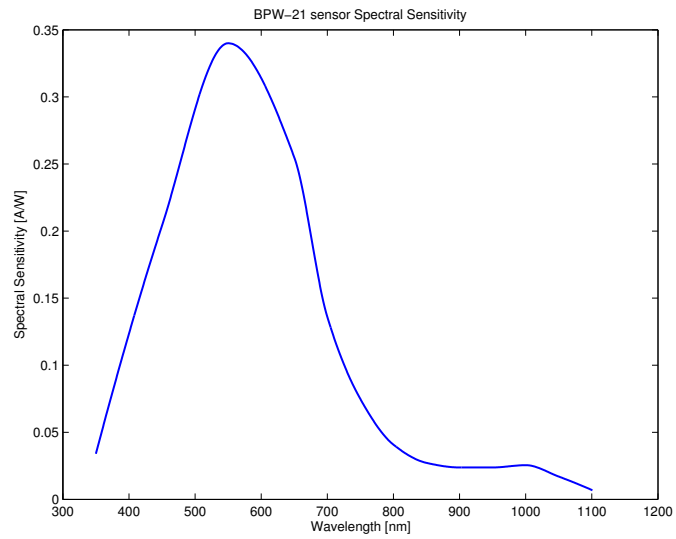

Figure 20: Spectral Sensitivity for BWP-21

Sun irradiance.

$$I_{p,Sun}(\varphi) = S_{rel}(\varphi) * ActiveArea * \sum_{i=1}^{n}(PowerDensity(\lambda_i) * SpectralSensitivity(\lambda_i) * \Delta\lambda) \quad (4)$$

Where,
$\Delta\lambda = \lambda_{i+1} - \lambda i$
$Active\ area\ of\ sensor = 7.34 * 10^{-6} m^2$

$$\sum_{i=1}^{n}(PowerDensity(\lambda_i) * SpectralSensitivity(\lambda_i) * \Delta\lambda) = 158.92\ [A/m^2]$$

This value is calculated from the Sun irradiance AM0 ASTM-E-490 data. This data can be downloaded from [13]. Using the same procedure described in section 3.1.1 S_{rel} depends on the angle of irradiation, shown in figure 15, different S_{rel} values at different angles possible are tabulated in Table 10.
Let us consider $\varphi = 0°$

$$I_{p,Sun}(0) = 1 * 7.34 * 10^{-6} m^2 * 158.92 = 1.17 * 10^{-3}\ [A]$$

Considering the temperature of sensor $= 50°C$

$$I_d(50°C) \ = 8 * 10^{-12}\ [A]$$

BPW-21 sensor can be connected in two modes, namely, Biased and Unbiased, for PilsenCube ADS BPW-21 is connected in unbiased mode, so the dark current for lower voltage is considered. Refer data sheet A.2.2 Using equation 2 Total noise current is calculated.
where,

$$
\begin{aligned}
ShotNoiseI_S &= \sqrt{2 * q * I_d * B} \\
&= \sqrt{2 * 1.6 * 10^{-19} * 8 * 10^{-12} * 10} \\
&= 5.06 * 10^{-14}\ [A] \\
ThermalNoiseI_T &= \sqrt{\frac{4 * k_b * T * B}{R_{SH}}} \\
&= \sqrt{\frac{4 * 1.38 * 10^{-23} * 323 * 10}{4 * 10^4}} \\
&= 2.11 * 10^{-12}\ [A] \\
\therefore I_{totalnoise} &= 2.11 * 10^{-12}\ [A] \\
SNR_{db} &= 20 * Log\left(\frac{I_p}{I_{totalnoise}}\right) \\
&= 20 * Log\left(\frac{1.17 * 10^{-3}}{2.11 * 10^{-12}}\right) \\
&= 175db
\end{aligned}
$$

All the calculated photocurrents as a function of irradiation angle are tabulated in Table 10.

3.2.2 BPW-21 in Albedo Irradiation

In this section output signals of BPW-21 in Earth Albedo are calculated. Only a sample calculation is provided, with 0° to 90° irradiance angle are tabulated. figure 18 details all the angles with respect to Earth Albedo irradiance.

$$
I_{p,Albedo}(\varphi) = S_{mean}(\varphi) * ActiveArea * \sum_{i=1}^{n}(0.3 * PowerDensity(\lambda_i) * SpectralSensitivity(\lambda_i) * \Delta\lambda) \quad (5)
$$

$$
\sum_{i=1}^{n}(0.3 * PowerDensity(\lambda_i) * SpectralSensitivity(\lambda_i) * \Delta\lambda) = 47.676\ [A/m^2]
$$

S_{mean} depends on the angle of irradiation and Earth disc, the figure 15 shows the responsivity of the sensor, different S_{mean} values at different angles possible are tabulated in Table 10.

Let us consider $\varphi = 0°$

$$
S_{mean}(0) = \frac{(1_{(0°)} + 2 * 0.995_{(\pm 5°)} + 2 * 0.99_{(\pm 10°)} + 2 * 0.98_{(\pm 15°)} + ...)}{27} = 0.76
$$

$$
I_{p,Albedo}(0) = 0.76 * 7.34 * 10^{-6} m^2 * 47.676 = 2.66 * 10^{-4}\ [A]
$$

Considering the Total Noise of sensor at 50° and using the Total noise current $I_{totalNoise}$ values from the section 3.2.1, SNR values can be calculated.

$$
\begin{aligned}
SNR_{db} &= 20 * Log\left(\frac{I_p}{I_{totalnoise}}\right) \\
&= 20 * Log\left(\frac{2.66 * 10^{-4}}{2.11 * 10^{-12}}\right) \\
&= 162db
\end{aligned}
$$

3.3 Infrared Radiation sensor TPS-230

TPS-230 sensors are used in the contactless thermometer. The measured object should fill the sensor field of view to obtain accurate temperature measurement. For example if the object temperature is 25°C and if the object is large enough to cover the most sensitive part of the field of view, then the sensor will measure 25°C. If the sensor field of view is partly covered by the object with temperature T1 and partly by another object with temperature T2 then the measured temperature will be in between T1 and T2 in relation to the sensor sensitivity in the direction of the object. Similarly if the sensor field of view is partly covered by the Earth at 15°C and partly covered by the free space at -270°C, then the measured temperature will be the weighted mean value.

3.3.1 TPS-230 in Sun Thermal Radiation

TPS-230 sensor will not detect Sun, due to its high temperature (5500°C) the spectrum band is out of sensor sensitivity. Also the Sun disc is visible under low angle (0.5°) in comparison to the sensor field of view. Also the thermosphere temperature is not detectable. As TPS-230 is a contactless thermometer it should detect the high temperatures when pointed towards sky from the ground.

3.3.2 TPS-230 in Earth Thermal Emission

In this section output signals of TPS-230 in Earth thermal radiation are calculated. Only a sample calculation is provided, figure 23 details all the angles with respect to Earth Thermal Emission. From figure 3 in datasheet A.2.3 the relative directional sensitivity as a function of irradiance angle is obtained. *Let us consider* $\varphi = 0°$

$$WeightsSum = \sum_{i=1}^{n}(SpectralSensitivity(\lambda_i)) = 16.0376$$

Weighted Temperature,

$$T_{weighted} = \frac{T_{Obj}}{WeightsSum} * ((1_{(0°)} + 2 * 0.995_{(\pm 5°)} + 2 * 0.99_{(\pm 10°)} + 2 * 0.98_{(\pm 15°)} + ...)) + \frac{T_{freeSpace}}{WeightedSum} * (2 * 0.05_{(\pm 80°)} + .) = 13.74°C$$

For simplicity of calculation the sensor ambient temperature is assumed to be constant at 25°C, in satellite ADCS software will compensate this with the true ambient temperature measured by internal thermistor. Using the figure 21 and comparing the calculated weighted temperature with the object temperature, output voltage can be obtained. In our case the corresponding output voltage for 13.74°C is -0.2967[mV].

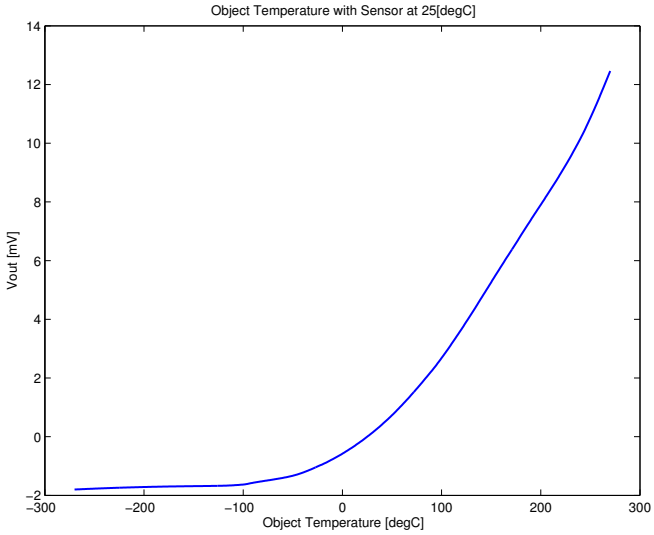

Figure 21: Ratio of TPS sensor

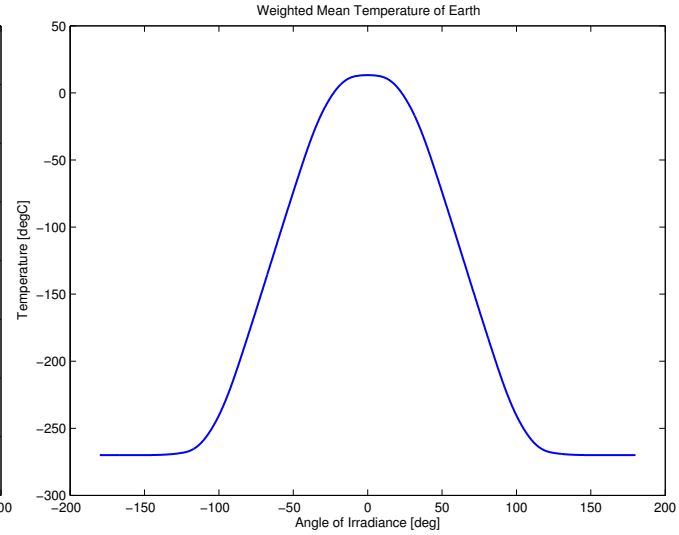

Figure 22: Ratio of TPS sensor

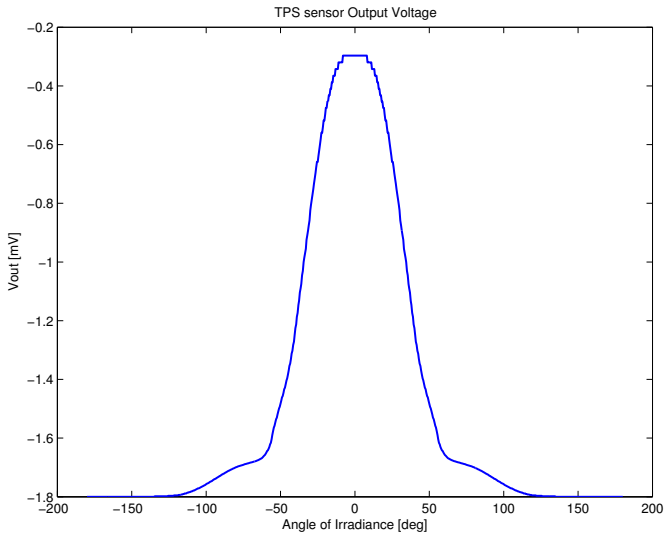

Figure 23: Output Voltage

Angle of Irradiance	**SNR [db] at 25°C**
0	147.00
5	147.00
10	148.00
15	150.00
20	152.00
25	154.00
30	156.00
35	158.00
40	160.00
45	161.00
50	161.00
55	162.00
60	162.00
65	162.00
70	162.00
75	163.00
80	163.00
85	163.00
90	163.00

Table 15: SNR_{Albedo} in db of TPS-230 sensor

4 Simulation Results

In this section the sensor output during the satellite rotation with several relative position of Earth and Sun are documented. The sensors EPD-365 and BPW-21 are used for Sun position determination and TPS-230 is used for Earth position determination. The Simulated ratio plots are shown in figure 27, figure 26 and figure 25.

Pico satellite in Earth Shadow

When satellite is in Earth shadow only the TPS-230 sensor will have signal. As the other two sensors (BPW-21 and EPD-365) are depended on solar radiation due to which they will only have noise. The highest temperature will be measured by the TPS-230 sensor on the x side refer figure 24 for sides specification. Now considering the neighboring sides the sensors on -y side and -z side will measure the next two high temperatures. For example the Ratio -x/-y = 0.1591 and Ratio -x/-z = 0.175, then azimuth can be found from the figure 25 which is 0° and elevation of -10°. Thus determining the Earth positon.

Sun and Earth are visible by different Sensors

In this condition, let us consider the side +x is pointing directly towards Sun and -x is pointing towards the Earth. In this case both Sun and Earth position can be determined. First consider the EPD-365 and BPW-21 sensors, as the Sun can be interpreted as point source the sides at 90° from +x will only give noise. So in this case ratios are calculated between maximum current and noise. For example consider EPD-365 with Ratio +x/+y = 1.633E08 and ratio +x/+z = 1.633E08 then there corresponding angles can be obtained from the figure 26 we get the angles as azimuth as 0° and elevation as 90°.

Similarly we get almost same angles from the BPW-21 sensor for the measured photocurrent ratios. Then these two pairs are averaged to obtain the Sun position.

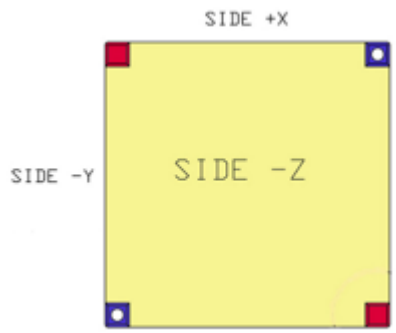

Figure 24: Sides of the CubeSat

Now considering the TPS-230 sensor, which is on -x side will have maximum value so the ratios -x/-y and -x/-z are obtained from which corresponding azimuth and elevation angles are obtained.

Sun and Earth are visible by same Sensors

In this condition all the sides are equally irradiated by Sun and Earth, so there ratios will be 1, comparing with the Figure 27 the angles obtained will be 45°. This is valid for all the sensors.

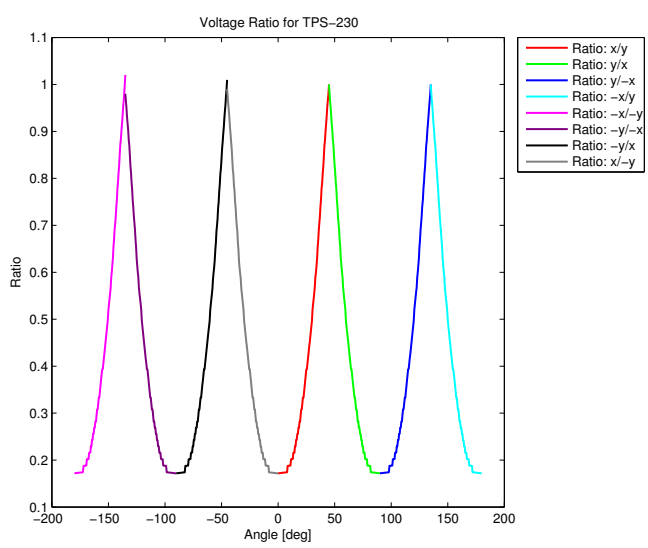

Figure 25: Ratio of TPS sensor

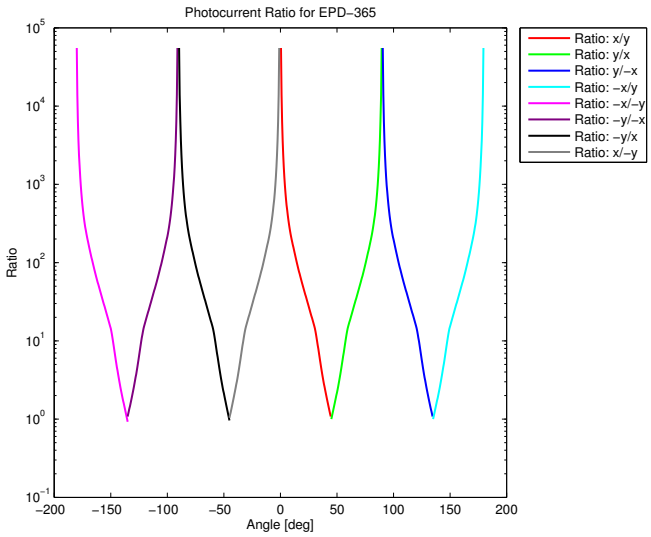

Figure 26: Ratio of BPW sensor

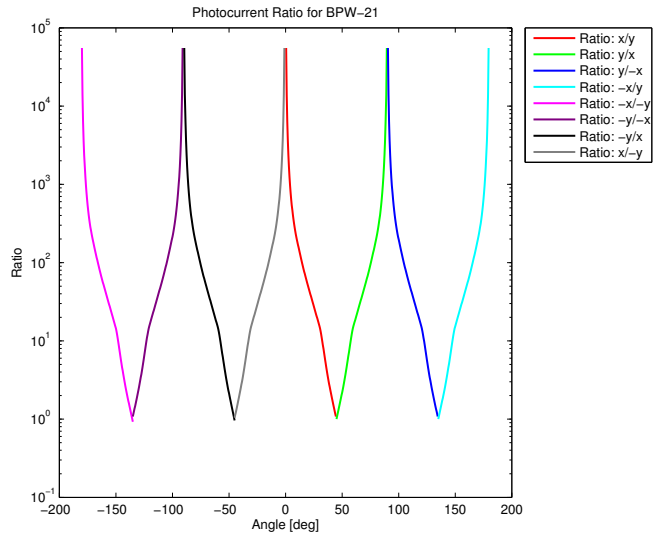

Figure 27: Ratio of BPW sensor

5 Algorithm

In this section a simple algorithm is proposed which is suitable for the low power ADCS computer and to estimate Sun and Earth position in satellite body coordinates. The flow chart in figure 28 gives the details of the procedure used for development of this algorithm. The threshold block determines an electronic terminator to each of the BPW and EPD sensors to activate or deactivate them. The basic termination can be when satellite is fully lite, at Gibbous, at Half lite, at Crescent and in Dark. For PilsenCube these terminators are modeled in between Crescent and Dark for power saving and in between Dark and Crescent for initiating solar cells orientation towards Sun. The implementation of terminators is out of scope of this thesis.
Let us consider the following measurements from the sensors with subscript signifying the side of the satellite. EPD and BPW sensors measure Photocurrent [A] and TPS sensor measure temperature and gives Photovoltage [mV].

$$epd_{+x}, epd_{+y}, epd_{+z}, epd_{-x}, epd_{-y}, epd_{-z}$$

$$bpw_{+x}, bpw_{+y}, bpw_{+z}, bpw_{-x}, bpw_{-y}, bpw_{-z}$$

$$tps_{+x}, tps_{+y}, tps_{+z}, tps_{-x}, tps_{-y}, tps_{-z}$$

Considering the TPS sensor as it cannot measure the high temperatures of the Sun and thermosphere, the TPS sensors pointing towards the Sun will have some noise which is assumed to be lower that the readings from the Earth side sensors. Let us assume the sides +x, -y, -z are pointing towards Sun and -x, +y, +z are pointing towards Earth and arranging in the matrix from we get,

$$tps_{meas} = [tps_{+x}\ tps_{+y}\ tps_{+z}\ tps_{-x}\ tps_{-y}\ tps_{-z}] \tag{6}$$

$$bpw_{meas} = [bpw_{+x}\ bpw_{+y}\ bpw_{+z}\ bpw_{-x}\ bpw_{-y}\ bpw_{-z}] \tag{7}$$

$$epd_{meas} = [epd_{+x}\ epd_{+y}\ epd_{+z}\ epd_{-x}\ epd_{-y}\ epd_{-z}] \tag{8}$$

Let us assume +x is pointing towards Sun at normal then as the sensors on the -y and -z are at 90° are not irradiated, but on the other hand when -x is pointing towards Earth, from 700 km the Earth disk irradiates 5 TPS sensors so expect +x all other sides are irradiated by Earth albedo. Let us consider TPS sensor measurement from equation 6 and sorting it with highest value first and pairing the most irradiated sides together, we obtain (here only the highest 3 values are of interest).

$$tps_{Meas} = [tps_{-x}\ tps_{+y}\ tps_{+z}\ tps_{-y}\ tps_{-z}\ tps_{+x}] \tag{9}$$

Now considering the highest value as reference the ratios are calculated between the pair of neighboring sensors,

$$tps_{Ratio_1} = \frac{tps_{-x}}{tps_{+y}} \tag{10}$$

$$tps_{Ratio_2} = \frac{tps_{-x}}{tps_{+z}} \tag{11}$$

Comparing the ratios from equation 12 and 13 with the pre-calculated lookup table (LUT), two angles of Earth position in satellite body reference frame are obtained. α_1 is the azimuth angle of the Earth and α_2 is the elevation of the Earth. Thus determining the Earth position.

$$\alpha_1 = LUT\left(\frac{tps_{-x}}{tps_{+y}}\right) \tag{12}$$

$$\alpha_2 = LUT\left(\frac{tps_{-x}}{tps_{+z}}\right) \tag{13}$$

Now let us consider EPD and BPW sensors to determine the Sun position. Here the sensors need albedo correction, as all the sides except the side directly pointing the Sun have albedo photocurrent added to their measurement. This can be compensated from determination of Earth position and find the sides that needs to be corrected to obtain accuracy in Sun position determination. From equation 9 the sides -y and -z are the sides that needs correction, as these sides are the lowest values and side +x is not considered as it gives noise which is assumed to be the lowest and pointing towards Sun. The correction equations are given below,

$$bpw_{-y,corrected} = bpw_{-y,meas} - bpw_{-y,cal.albedo(\alpha1,\alpha2)}$$

$$bpw_{-z,corrected} = bpw_{-z,meas} - bpw_{-z,cal.albedo(\alpha1,\alpha2)}$$

$$epd_{-y,corrected} = epd_{-y,meas} - epd_{-y,cal.albedo(\alpha1,\alpha2)}$$

$$epd_{-z,corrected} = epd_{-z,meas} - epd_{-z,cal.albedo(\alpha1,\alpha2)}$$

Considering these corrections and sorting the matrix with highest value first and pairing the neighboring sides together, matrix 7 can be written as,

$$bpw_{meas} = [bpw_{+x}\ bpw_{-y,corrected}\ bpw_{-z,corrected}\ bpw_{-x}\ bpw_{-y}\ bpw_{-z}] \tag{14}$$

$$epd_{meas} = [epd_{+x}\ epd_{-y,corrected}\ epd_{-z,corrected}\ epd_{-x}\ epd_{+y}\ epd_{+z}] \tag{15}$$

Considering the highest value as reference for the BPW and EPD sensor, Ratios can be calculated.

$$\therefore bpw_{Ratio_1} = \frac{bpw_{+x}}{bpw_{-y,corrected}} \tag{16}$$

$$bpw_{Ratio_2} = \frac{bpw_{+x}}{bpw_{-z,corrected}} \tag{17}$$

$$epd_{Ratio_1} = \frac{epd_{+x}}{epd_{-y,corrected}} \tag{18}$$

$$epd_{Ratio_2} = \frac{epd_{+x}}{epd_{-z,corrected}} \tag{19}$$

Comparing these ratios with the lookup table values we obtain the required azimuth and elevation angles of the Sun.

$$\alpha_{31} = LUT\left(\frac{bpw_{+x}}{bpw_{-y,corrected}}\right) \tag{20}$$

$$\alpha_{32} = LUT\left(\frac{bpw_{+x}}{bpw_{-z,corrected}}\right) \tag{21}$$

$$\alpha_{41} = LUT\left(\frac{epd_{+x}}{epd_{-y,corrected}}\right) \tag{22}$$

$$\alpha_{42} = LUT\left(\frac{epd_{+x}}{epd_{-z,corrected}}\right) \tag{23}$$

Now we obtain four angles here, taking average of the corresponding sides we obtain the Sun position in satellite body fixed reference frame.Thus Sun position is determined.

$$\alpha_3 = \left(\frac{\alpha_{31} + \alpha_{41}}{2}\right) \tag{24}$$

$$\alpha_4 = \left(\frac{\alpha_{32} + \alpha_{42}}{2}\right) \tag{25}$$

6 Conclusion

From the analysis and simulations only TPS-230 Infrared sensor is sufficient to estimate the Earth position, irrespective of the fact that EPD-365 Ultraviolet sensor has acceptable SNR ratio, as per the authors understanding the backscattered UV radiation from the Earth depends on constantly varying factors like Albedo, UV absorption by ozone layer and UV radiation behavior on high solar activity days, which may arise inconsistency in the measurement, due to which UV sensor and visible radiation sensors are used for Sun position determination. From theoretical calculation and simulation carried out in this thesis, illustrate that it is possible to use optical sensors for ADS, which will probably be a low cost, low power solution for the CubeSat class.

7 Future work

More research has to be carried out on Earth backscattered UV radiation, which can contribute to the EPD-365 sensor and achieve better accuracy in Sun and Earth position estimation. These sensors are yet to be flown on PilsenCube Pico satellite, to discover exact behavior of the sensors.

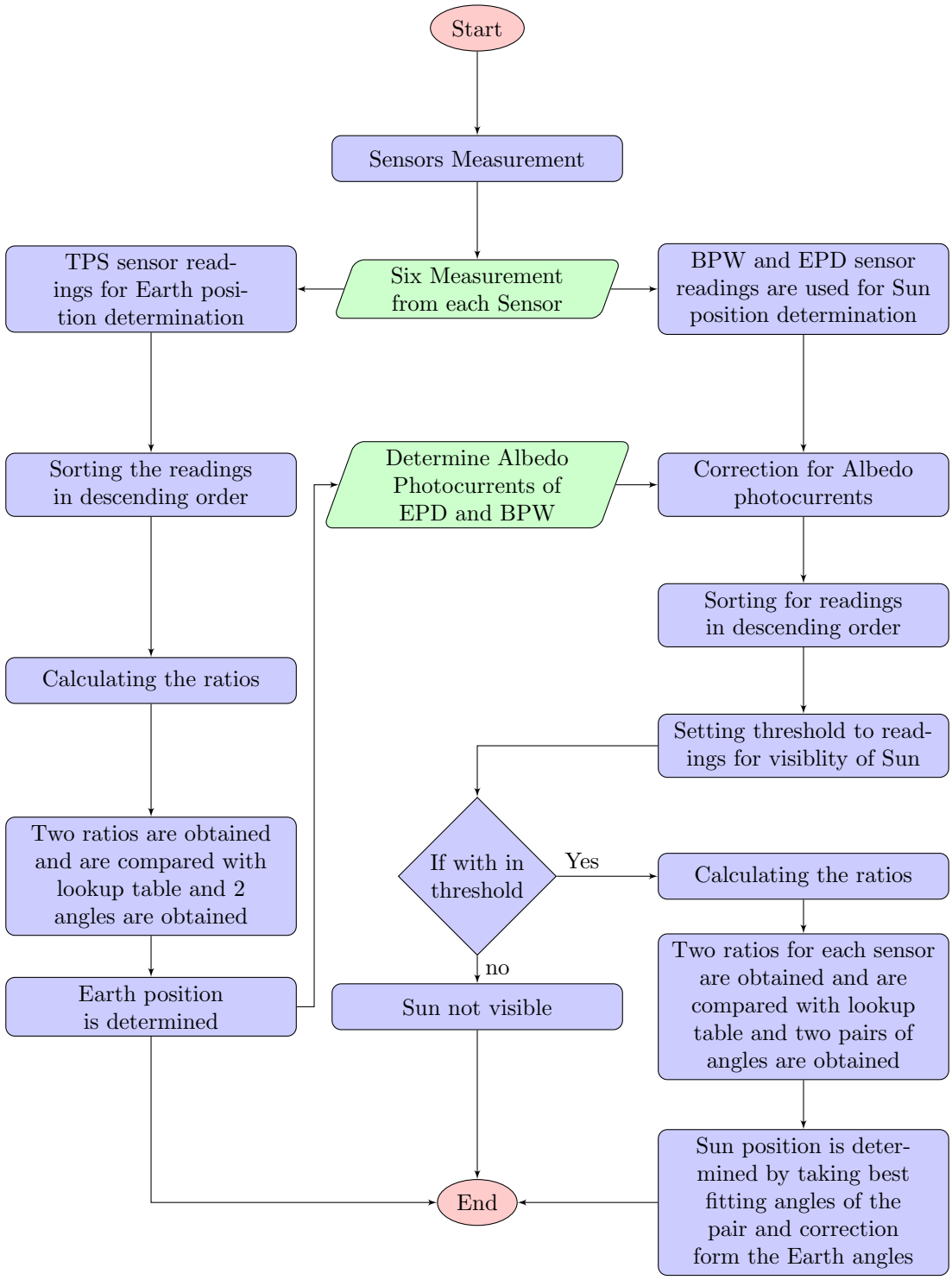

Figure 28: Flow Chart

References

[1] Armen Toorian, Emily Blundell, Jordi Puig Suari and Robert Twiggs, *CubeSats as Responsive Satellites*. AIAA 3_{rd} Responsive Space Conference, Long Beach , 2005.

[2] Phil Newman, *Diagram of a Solar-Type Star*. NASA Goddard Space Flight Center, 1997-2012.

[3] John Kennewell and Andrew McDonald, *The Solar Constant*. IPS Radio and Space Services.

[4] Helen Amanda Fricker, *Thermal Radiation*. Satellite Remote Sensing SIO 135/SIO 236.

[5] Amanda Briney, *Solar Radiation and the Earth's Albedo*. $http : //geography.about.com/od/physicalgeography/a/solarradiation.htm$

[6] Frank van Mierlo and Vaclav Smil, *Energy at the crossroads*. MIT Press, 2003.

[7] Hannes Grobe, *Albedo - Percentage of reflected Sun light in relation to the various surface condiditions of the Earth*. Creative Commons By-SA licence, 2006, $http : //en.wikipedia.org/wiki/File : Albedo - e_hg.svg$

[8] A.Acra, M.Jurdi, H.Mu'allem, Y.Karahagopian and Z.Raffoul, *Water Disinfection by Solar Radiation*. International Development Research Center, Canada, 1990. $http : //almashriq.hiof.no/lebanon/600/610/614/solar - water/idrc/01 - 09.html$

[9] C.R.Nave, *Hyper Physics*. Department of Physics and Astronomy, Georgia State University, 2012. $http : //hyperphysics.phy - astr.gsu.edu/hbase/ems1.html\#c1$

[10] Franz' Place, *Solar cells - Generating Electric Energy from Light*. $http : //www.superstrate.net/pv/irradiation/spectrum.html$

[11] Tracy DeLiberty, *Introduction to Environmental Remote Sensing*, Department of Geography, University of Delaware, 1999. $http : //www.udel.edu/Geography/DeLiberty/Geog474/geog474_energy_interact.html$

[12] Filip Tavernier and Michiel Steyaert, *High-Speed Optical Receivers with Integrated Photodiode in Nanoscale CMOS Springer*, Chapter-3, ISBN 1-4419-9924-8, 2011.

[13] Daryl Myer, *Solar Spectra: Standard Air Mass Zero*, ASTM-E-490-00, NREL, U.S. Department of Energy, 2004. $http : //rredc.nrel.gov/solar/spectra/am0/ASTM2000.html$

[14] Hilsenrath E, *Atmosheric Laboratory for Applications and Science*, NASA Goddard Space Flight Center,1996. $http : //mirador.gsfc.nasa.gov/$

[15] James R.Wertz, *Spacecraft Attitude Determination and Control*, Kluwer Academic Publishers, London, 1990.

A Appendix

A.1 Matlab Code

```
%%%%%%%%%% MATLAB CODE for PilsenCube Pico Satellite Optical ADS %%%%%%%%%

%   Master Thesis
%   Author          : Nagarjuna Rao Kandimalla
%   Submission Date : 18/May/2012

%%%%%%%%%%%%%%%%%%%%%%%%%%%%%%%%%%%%%%%%%%%%%%%%%%%%%%%%%%%%%%%%%%%%%%%%%%%%%%%%

clear all; close all;
%% Importing Data from Sun AM0 Irradiance and SBUV
d = importdata('dataAM0SBUV.txt','\t',1);
data = d.data;

wavelengthU=[240 250 260 270 280 300 350 365 380 390 400 410];
responsivityU=[0.00002 0.0009 0.008 0.02 0.03 0.05 0.068 0.07 0.04 0.01 0.00015 0.000001];

wavelengthV=[350 450 550 650 700 750 800 850 900 950 1000 1050 1101];
responsivityV=[0.034 0.204 0.34 0.255 0.136 0.0748 0.0408 0.0272 0.0238 0.0238 0.0255 0.017 ↩
    0.0068];

wavelengthUV = 240:1:411;
wavelengthVis = 350:1:1101;

powerDensitySBUV = interp1(data(1:172,4),data(1:172,5),wavelengthUV,'pchip');
responsivitySBUV = interp1(wavelengthU,responsivityU,wavelengthUV,'pchip');

powerDensityUVAM0 = interp1(data(1:172,1),data(1:172,2),wavelengthUV,'pchip');
responsivityUVAM0 = interp1(wavelengthU,responsivityU,wavelengthUV,'pchip');

powerDensityVisAM0 = interp1(data(1:488,7),data(1:488,8),wavelengthVis,'pchip');
responsivityVisAM0 = interp1(wavelengthV,responsivityV,wavelengthVis,'pchip');
%% scientific Constants
q = 1.6E-19;
B = 10;
Kb = 1.38E-23;
%% EPD-365 Sensor Data
epdRsh = 2E11;
epdActiveArea = 1.2E-6;
epdPowerSun = 0;
epdPowerAlbedo = 0;

angle = [-90 -80 -60 -40 -20 0 20 40 60 80 90];
senRel = [0 0.005 0.05 0.5 0.95 1 0.95 0.5 0.05 0.005 0];
epdAngle = -90:0.5:90;
Srel = interp1(angle, senRel, epdAngle, 'pchip');
epdSrel = [transpose([(-180:0.5:-90.5) epdAngle (90.5:0.5:180)]),transpose([zeros(1,180) ↩
    Srel zeros(1,180)])];

angle = [-180 -155 -150 -135 -90 -45 -5 0 5 45 90 135 150 155 180];
senMean = [0 0 0.0003 0.0037 0.22 0.55 0.76 0.76 0.76 0.55 0.22 0.0037 0.0003 0 0];
angleSmean = -180:0.5:180;
Smean = interp1(angle, senMean, angleSmean, 'pchip');
epdSmean = [transpose(angleSmean),transpose(Smean)];

epdDataAM0 = [transpose(wavelengthUV),transpose(powerDensityUVAM0),transpose(↩
    responsivityUVAM0)];
epdDataSBUV = [transpose(wavelengthUV),transpose(powerDensitySBUV),transpose(↩
    responsivitySBUV)];
epdId = [25,5E-12;50,4E-10;75,4E-10;100,4E-10]; %epdId(Temp,Id)

%% Calculation for EPD-365
for i = 1:171
epdpowerAM0 = epdDataAM0(i,2)*epdDataAM0(i,3)*(epdDataAM0(i+1,1)-epdDataAM0(i,1));
epdPowerSun = epdPowerSun+epdpowerAM0;
epdpowerSBUV = 0.2290*epdDataAM0(i,2)*epdDataAM0(i,3)*(epdDataSBUV(i+1,1)-epdDataSBUV(i,1));
epdPowerAlbedo = epdPowerAlbedo+epdpowerSBUV;
end
for i = 1:length(epdSrel)
epdIpSun(i,1)= epdSrel(i,2)*epdActiveArea*epdPowerSun; %0.07 [A/W] is the peak responsivity
%epdIpAlbedo(i,1)= epdSmean(i,2)*epdActiveArea*epdPowerAlbedo;
end
for i = 1:length(epdSmean)
    epdIpAlbedo(i,1)= epdSmean(i,2)*epdActiveArea*epdPowerAlbedo;
end
for i = 1:4
    epdIs(i,1) = sqrt(2 * q * epdId(i,2) * B);
    epdIt(i,1) = sqrt((4*Kb* (epdId(i,1)+273) *B)/epdRsh);
    epdITotN(i,1) = sqrt(epdIs(i,1)^2 + epdIt(i,1)^2);
    for j = 1:length(epdSrel)
        epdSnrSun(j,i) = 20*log10(epdIpSun(j,1)/epdITotN(i,1));
        %epdSnrAlbedo(j,i) = 20*log10(epdIpAlbedo(j,1)/epdITotN(i,1));
```

```
    end
    for k = 1:length(epdSmean)
        epdSnrAlbedo(k,i) = 20*log10(epdIpAlbedo(k,1)/epdITotN(i,1));
    end
end

epdSnrSun = round(epdSnrSun);
epdSnrAlbedo = round(epdSnrAlbedo);

epdIpSun(:,2) = epdSrel(:,1);
epdIpAlbedo(:,2) = epdSmean(:,1);

epdIpSun_plus_x=epdIpSun;
epdIpSun_plus_y(:,2)=epdIpSun(:,2);
epdIpSun_minus_x(:,2)=epdIpSun(:,2);
epdIpSun_minus_y(:,2)=epdIpSun(:,2);

epdIpSun_plus_y(:,1)=circshift(epdIpSun(:,1),[180 0]);
epdIpSun_minus_x(:,1)=circshift(epdIpSun(:,1),[360 0]);
epdIpSun_minus_y(:,1)=circshift(epdIpSun(:,1),[540 0]);

epdIpAlbedo_plus_x=epdIpAlbedo;
epdIpAlbedo_plus_y(:,2)=epdIpAlbedo(:,2);
epdIpAlbedo_minus_x(:,2)=epdIpAlbedo(:,2);
epdIpAlbedo_minus_y(:,2)=epdIpAlbedo(:,2);

epdIpAlbedo_plus_y(:,1)=circshift(epdIpAlbedo(:,1),[180 0]);
epdIpAlbedo_minus_x(:,1)=circshift(epdIpAlbedo(:,1),[360 0]);
epdIpAlbedo_minus_y(:,1)=circshift(epdIpAlbedo(:,1),[540 0]);

figure(1);
%plot(epdSrel(:,1), epdIpSun(:,1));
plot(epdIpSun_plus_x(:,2), epdIpSun_plus_x(:,1),'r','LineWidth',1.5);
hold on;
plot(epdIpSun_plus_y(:,2), epdIpSun_plus_y(:,1),'b','LineWidth',1.5);
plot(epdIpSun_minus_x(:,2), epdIpSun_minus_x(:,1), 'g','LineWidth',1.5);
plot(epdIpSun_minus_y(:,2), epdIpSun_minus_y(:,1), 'k','LineWidth',1.5);
title('EPD-365 sensor Sun AM0 irradiance');
xlabel('Angle of irradiance [degrees]');
ylabel('Photocurrent [ A ]');
epdIpLegend=legend('Side: x','Side: y ','Side: -x','Side: -y');
set(epdIpLegend,'Location','NorthEastOutside')
hold off;
print -depsc ../Latex/Thesis/epdIpSun
figure(2);
%plot(epdSmean(:,1), epdIpAlbedo);
plot(epdIpAlbedo_plus_x(:,2), epdIpAlbedo_plus_x(:,1),'r','LineWidth',1.5);
hold on;
plot(epdIpAlbedo_plus_y(:,2), epdIpAlbedo_plus_y(:,1),'b','LineWidth',1.5);
plot(epdIpAlbedo_minus_x(:,2), epdIpAlbedo_minus_x(:,1), 'g','LineWidth',1.5);
plot(epdIpAlbedo_minus_y(:,2), epdIpAlbedo_minus_y(:,1), 'k','LineWidth',1.5);
title('EPD-365 sensor Earth Albedo irradiance');
xlabel('Angle of irradiance [degrees]');
ylabel('Photocurrent [ A ]');
epdIpALegend=legend('Side: x','Side: y ','Side: -x','Side: -y');
set(epdIpALegend,'Location','NorthEastOutside')
hold off;
print -depsc ../Latex/Thesis/epdIpAlbedo
figure(3)
semilogy(epdIpSun(361:450,2),epdIpSun_plus_x(361:450,1)./epdIpSun_plus_y(361:450,1),'r','↩
    LineWidth',1.5);
hold on;
semilogy(epdIpSun(451:540,2),epdIpSun_plus_y(451:540,1)./epdIpSun_plus_x(451:540,1),'g','↩
    LineWidth',1.5);
hold on;
semilogy(epdIpSun(541:630,2),epdIpSun_plus_y(541:630,1)./epdIpSun_minus_x(541:630,1),'b','↩
    LineWidth',1.5);
hold on;
semilogy(epdIpSun(631:721,2),epdIpSun_minus_x(631:721,1)./epdIpSun_plus_y(631:721,1),'c','↩
    LineWidth',1.5);
hold on;
semilogy(epdIpSun(1:91,2),epdIpSun_minus_x(1:91,1)./epdIpSun_minus_y(1:91,1),'m','LineWidth'↩
    ,1.5);
hold on;
semilogy(epdIpSun(91:181,2),epdIpSun_minus_y(91:181,1)./epdIpSun_minus_x(91:181,1),'color'↩
    ,[0.5 0 0.5],'LineWidth',1.5);
hold on;
semilogy(epdIpSun(181:271,2),epdIpSun_minus_y(181:271,1)./epdIpSun_plus_x(181:271,1),'k','↩
    LineWidth',1.5);
hold on;
```

```
semilogy(epdIpSun(271:361,2),epdIpSun_plus_x(271:361,1)./epdIpSun_minus_y(271:361,1),'color'↩
    ,[0.5 0.5 0.5],'LineWidth',1.5);
title('Photocurrent Ratio for EPD-365');
xlabel('Angle [deg]');
ylabel('Ratio');
tpsLegend=legend('Ratio: x/y','Ratio: y/x ','Ratio: y/-x','Ratio: -x/y','Ratio: -x/-y','↩
    Ratio: -y/-x','Ratio: -y/x','Ratio: x/-y');
set(tpsLegend,'Location','NorthEastOutside');
hold off;
print -depsc ../Latex/Thesis/epdIpRatioSun
%% BPW-21 Sensor Data
bpwDataAM0 = [transpose(wavelengthVis),transpose(powerDensityVisAM0),transpose(↩
    responsivityVisAM0)];
bpwSrel = [epdSrel(:,1),epdSrel(:,2)];
bpwSmean = [epdSmean(:,1),epdSmean(:,2)];
bpwPowerSun = 0;
bpwPowerAlbedo = 0;
bpwActiveArea = 7.34E-6;
bpwRsh = 40000;
bpwId = [25,8E-12;50,8E-12;75,8E-12;100,8E-12];

%% Calculation for BPW-21
for i = 1:751
bpwPowerAM0 = bpwDataAM0(i,2)*bpwDataAM0(i,3)*(bpwDataAM0(i+1,1)-bpwDataAM0(i,1));
bpwPowerSun = bpwPowerSun+bpwPowerAM0;
bpwPowerAM = 0.3*bpwDataAM0(i,2)*bpwDataAM0(i,3)*(bpwDataAM0(i+1,1)-bpwDataAM0(i,1));
bpwPowerAlbedo = bpwPowerAlbedo+(bpwPowerAM);
end
for i = 1:length(bpwSrel)
bpwIpSun(i,1)= bpwSrel(i,2)*bpwActiveArea*bpwPowerSun;
%bpwIpAlbedo(i,1)= 0.3*bpwSmean(i,2)*bpwActiveArea*bpwPowerAlbedo;
end
for i = 1:length(bpwSmean)
    bpwIpAlbedo(i,1)= bpwSmean(i,2)*bpwActiveArea*bpwPowerAlbedo;
end
for i = 1:4
    bpwIs(i,1) = sqrt(2 * q * bpwId(i,2) * B);
    bpwIt(i,1) = sqrt((4*Kb* (bpwId(i,1)+273) *B)/bpwRsh);
    bpwITotN(i,1) = sqrt(bpwIs(i,1)^2 + bpwIt(i,1)^2);
    for j = 1:length(bpwSrel)
        bpwSnrSun(j,i) = 20*log10(bpwIpSun(j,1)/bpwITotN(i,1));
        %bpwSnrAlbedo(j,i) = 20*log10(bpwIpAlbedo(j,1)/bpwITotN(i,1));
    end
    for k = 1:length(bpwSmean)
    bpwSnrAlbedo(k,i) = 20*log10(bpwIpAlbedo(k,1)/bpwITotN(i,1));
    end
end
bpwSnrSun = round(bpwSnrSun);
bpwSnrAlbedo = round(bpwSnrAlbedo);

bpwIpSun(:,2) = bpwSrel(:,1);
bpwIpAlbedo(:,2) = bpwSmean(:,1);

bpwIpSun_plus_x=bpwIpSun;
bpwIpSun_plus_y(:,2)=bpwIpSun(:,2);
bpwIpSun_minus_x(:,2)=bpwIpSun(:,2);
bpwIpSun_minus_y(:,2)=bpwIpSun(:,2);

bpwIpSun_plus_y(:,1)=circshift(bpwIpSun(:,1),[180 0]);
bpwIpSun_minus_x(:,1)=circshift(bpwIpSun(:,1),[360 0]);
bpwIpSun_minus_y(:,1)=circshift(bpwIpSun(:,1),[540 0]);

bpwIpAlbedo_plus_x=bpwIpAlbedo;
bpwIpAlbedo_plus_y(:,2)=bpwIpAlbedo(:,2);
bpwIpAlbedo_minus_x(:,2)=bpwIpAlbedo(:,2);
bpwIpAlbedo_minus_y(:,2)=bpwIpAlbedo(:,2);

bpwIpAlbedo_plus_y(:,1)=circshift(bpwIpAlbedo(:,1),[180 0]);
bpwIpAlbedo_minus_x(:,1)=circshift(bpwIpAlbedo(:,1),[360 0]);
bpwIpAlbedo_minus_y(:,1)=circshift(bpwIpAlbedo(:,1),[540 0]);

figure(4)
plot(wavelengthVis, responsivityVisAM0,'LineWidth',1.5);
title('BPW-21 sensor Spectral Sensitivity');
xlabel('Wavelength [nm]');
ylabel('Spectral Sensitivity [A/W]');
print -depsc ../Latex/Thesis/bpwSensitivity;
figure(5);
%plot(bpwSrel(:,1), bpwIpSun(:,1));
plot(bpwIpSun_plus_x(:,2), bpwIpSun_plus_x(:,1),'r','LineWidth',1.5);
hold on;
```

```
plot(bpwIpSun_plus_y(:,2), bpwIpSun_plus_y(:,1),'b','LineWidth',1.5);
plot(bpwIpSun_minus_x(:,2), bpwIpSun_minus_x(:,1), 'g','LineWidth',1.5);
plot(bpwIpSun_minus_y(:,2), bpwIpSun_minus_y(:,1), 'k','LineWidth',1.5);
title('BPW-21 sensor Sun AM0 irradiance');
xlabel('Angle of irradiance [degrees]');
ylabel('Photocurrent [ A ]');
bpwIpLegend=legend('Side: x','Side: y ','Side: -x','Side: -y');
set(bpwIpLegend,'Location','NorthEastOutside')
hold off;
print -depsc ../Latex/Thesis/bpwIpSun
figure(6);
%plot(bpwSmean(:,1), bpwIpAlbedo);
plot(bpwIpAlbedo_plus_x(:,2), bpwIpAlbedo_plus_x(:,1),'r','LineWidth',1.5);
hold on;
plot(bpwIpAlbedo_plus_y(:,2), bpwIpAlbedo_plus_y(:,1),'b','LineWidth',1.5);
plot(bpwIpAlbedo_minus_x(:,2), bpwIpAlbedo_minus_x(:,1), 'g','LineWidth',1.5);
plot(bpwIpAlbedo_minus_y(:,2), bpwIpAlbedo_minus_y(:,1), 'k','LineWidth',1.5);
title('BPW-21 sensor Earth Albedo irradiance');
xlabel('Angle of irradiance [degrees]');
ylabel('Photocurrent [ A ]');
bpwIpALegend=legend('Side: x','Side: y ','Side: -x','Side: -y');
set(bpwIpALegend,'Location','NorthEastOutside')
hold off;
print -depsc ../Latex/Thesis/bpwIpAlbedo
figure(7)
semilogy(bpwIpSun(361:450,2),bpwIpSun_plus_x(361:450,1)./bpwIpSun_plus_y(361:450,1),'r','↩
    LineWidth',1.5);
hold on;
semilogy(bpwIpSun(451:540,2),bpwIpSun_plus_y(451:540,1)./bpwIpSun_plus_x(451:540,1),'g','↩
    LineWidth',1.5);
hold on;
semilogy(bpwIpSun(541:630,2),bpwIpSun_plus_y(541:630,1)./bpwIpSun_minus_x(541:630,1),'b','↩
    LineWidth',1.5);
hold on;
semilogy(bpwIpSun(631:721,2),bpwIpSun_minus_x(631:721,1)./bpwIpSun_plus_y(631:721,1),'c','↩
    LineWidth',1.5);
hold on;
semilogy(bpwIpSun(1:91,2),bpwIpSun_minus_x(1:91,1)./bpwIpSun_minus_y(1:91,1),'m','LineWidth'↩
    ,1.5);
hold on;
semilogy(bpwIpSun(91:181,2),bpwIpSun_minus_y(91:181,1)./bpwIpSun_minus_x(91:181,1),'color'↩
    ,[0.5 0 0.5],'LineWidth',1.5);
hold on;
semilogy(bpwIpSun(181:271,2),bpwIpSun_minus_y(181:271,1)./bpwIpSun_plus_x(181:271,1),'k','↩
    LineWidth',1.5);
hold on;
semilogy(bpwIpSun(271:361,2),bpwIpSun_plus_x(271:361,1)./bpwIpSun_minus_y(271:361,1),'color'↩
    ,[0.5 0.5 0.5],'LineWidth',1.5);
title('Photocurrent Ratio for BPW-21');
xlabel('Angle [deg]');
ylabel('Ratio');
tpsLegend=legend('Ratio: x/y','Ratio: y/x ','Ratio: y/-x','Ratio: -x/y','Ratio: -x/-y','↩
    Ratio: -y/-x','Ratio: -y/x','Ratio: x/-y');
set(tpsLegend,'Location','NorthEastOutside');
hold off;
print -depsc ../Latex/Thesis/bpwIpRatioSun

%% TPS-230 Sensor Data

angle = [-90 -80 -60 -40 -20 0 20 40 60 80 90];
sensitivity = [0 0.005 0.05 0.5 0.95 1 0.95 0.5 0.05 0.005 0];
tpsAngle = -90:0.5:90;
tpsSensitivity = interp1(angle,sensitivity,tpsAngle,'pchip');
tpsSrel = [transpose([(-180:0.5:-90.5) tpsAngle (90.5:0.5:180)]),transpose([zeros(1,180) ↩
    tpsSensitivity zeros(1,180)])];
tempE=[-270.*ones(1,230) 15.*ones(1,261) -270.*ones(1,230)];

for i=1:361
weTeE(i)=(circshift(tempE,[0 i-1])*tpsSrel(:,2))/sum(tpsSrel(:,2));
end;
weTeE=[weTeE(end:-1:2) weTeE];
weightTempE(:,1) = transpose([(-180:0.5:-90.5) tpsAngle (90.5:0.5:180)]);
weightTempE(:,2) = weTeE;

temp0=[-270 -180 -160 -120 -100 -90 -50 -20 -10 0 20 25 30 50 90 100 120 160 180 240 ↩
    270];
Vout=[-1.80 -1.70 -1.69 -1.67 -1.63 -1.57 -1.33 -0.94 -0.77 -0.58 -0.13 0 0.13 0.73 2.24 ↩
    2.68 3.66 5.8 6.86 10.16 12.46];

xx = -270:1:270;
yy=interp1(temp0,Vout,xx,'pchip');
```

```
zz = [transpose(xx),transpose(yy)];

for i = 1:721
    for j = 1:541
        if( zz(j,1) == round(weightTempE(i,2)))
            VoutE(i,1) = weightTempE(i,1);
            VoutE(i,2) = zz(j,2);
        end
    end
end

VoutE_plus_x=VoutE;
VoutE_plus_y(:,1)=VoutE(:,1);
VoutE_minus_x(:,1)=VoutE(:,1);
VoutE_minus_y(:,1)=VoutE(:,1);

VoutE_plus_y(:,2)=circshift(VoutE(:,2),[180 0]);
VoutE_minus_x(:,2)=circshift(VoutE(:,2),[360 0]);
VoutE_minus_y(:,2)=circshift(VoutE(:,2),[540 0]);

figure(8);
plot(zz(:,1), zz(:,2),'LineWidth',1.5);
title('Object Temperature with Sensor at 25[degC]');
xlabel('Object Temperature [degC]');
ylabel('Vout [mV]');
%tpsLegend=legend('');
%set(tpsLegend,'Location','Best')
print -depsc ../Latex/Thesis/tpsVout25
figure(9);
plot(weightTempE(:,1), weightTempE(:,2),'LineWidth',1.5)
% plot(weightTempE(1:181,1), weightTempE(1:181,2),'r');
% hold on;
% plot(weightTempE(182:361,1), weightTempE(182:361,2),'b');
% plot(weightTempE(362:541,1), weightTempE(362:541,2), 'g');
% plot(weightTempE(541:721,1), weightTempE(541:721,2), 'k');
title('Weighted Mean Temperature of Earth');
xlabel('Angle of Irradiance [deg]');
ylabel('Temperature [degC]');
% wTempE=legend('Side: -y, -x','Side: x, -y ','Side: x, y','Side: y, -x');
% set(wTempE,'Location','Best')
% hold off;
print -depsc ../Latex/Thesis/weightTempE
figure(10);
plot(VoutE(:,1),VoutE(:,2),'LineWidth',1.5);
title('TPS sensor Output Voltage');
xlabel('Angle of Irradiance [deg]');
ylabel('Vout [mV]');
print -depsc ../Latex/Thesis/VoutE
figure(11)
plot(VoutE(361:451,1),VoutE_plus_x(361:451,2)./VoutE_plus_y(361:451,2),'r','LineWidth',1.5);
hold on;
plot(VoutE(451:541,1),VoutE_plus_y(451:541,2)./VoutE_plus_x(451:541,2),'g','LineWidth',1.5);
hold on;
plot(VoutE(541:631,1),VoutE_plus_y(541:631,2)./VoutE_minus_x(541:631,2),'b','LineWidth',1.5)↩
    ;
hold on;
plot(VoutE(631:721,1),VoutE_minus_x(631:721,2)./VoutE_plus_y(631:721,2),'c','LineWidth',1.5)↩
    ;
hold on;
plot(VoutE(1:91,1),VoutE_minus_x(1:91,2)./VoutE_minus_y(1:91,2),'m','LineWidth',1.5);
hold on;
plot(VoutE(91:181,1),VoutE_minus_y(91:181,2)./VoutE_minus_x(91:181,2),'color',[0.5 0 0.5],'↩
    LineWidth',1.5);
hold on;
plot(VoutE(181:271,1),VoutE_minus_y(181:271,2)./VoutE_plus_x(181:271,2),'k','LineWidth',1.5)↩
    ;
hold on;
plot(VoutE(271:361,1),VoutE_plus_x(271:361,2)./VoutE_minus_y(271:361,2),'color',[0.5 0.5 ↩
    0.5],'LineWidth',1.5);
title('Voltage Ratio for TPS-230');
xlabel('Angle [deg]');
ylabel('Ratio');
tpsLegend=legend('Ratio: x/y','Ratio: y/x ','Ratio: y/-x','Ratio: -x/y','Ratio: -x/-y','↩
    Ratio: -y/-x','Ratio: -y/x','Ratio: x/-y');
set(tpsLegend,'Location','NorthEastOutside');
hold off;
print -depsc ../Latex/Thesis/tpsVoRatioE

tpsSnrAlbedo = 0;
VoutN = 12.65E-09;
for i = 1:length(tpsSrel)
```

```
    tpsSnrAlbedo(i,1) = 20*log10(abs(VoutE(i,2))/VoutN);
end
tpsSnrAlbedo = round(tpsSnrAlbedo);

%% Latex conversion

FID = fopen('../Latex/Thesis/epdIp.tex', 'w');
fprintf(FID, '\\begin{tabular}{|m{2cm}|m{2.5cm}|m{2.5cm}|m{2.5cm}|m{2.5cm}|}\\hline \n');
fprintf(FID, '\\textbf{Angle of Irradiance } [deg]  & \\textbf{Relative Sensitivity} $S_{rel↩
    }$  & \\textbf{Photocurrent} $I_{P,Sun}$ [A] & \\textbf{Mean Sensitivity} $S_{mean}$    ↩
    & \\textbf{Photocurrent} $I_{P,Albedo}$ [A] \\\\ \\hline  \n');
i=361;
for k=1:19
    fprintf(FID, '%d & %6.3f & %8.2E & %6.3f & %8.2E \\\\ ', epdSrel(i,1),epdSrel(i,2), ↩
        epdIpSun(i,1), epdSmean(i,2), epdIpAlbedo(i,1));
    %if k==length(TC)
        fprintf(FID, '\\hline ');
    %end
    fprintf(FID, '\n');
    i=i+10;
end
fprintf(FID, '\\end{tabular}\n');
fclose(FID);

FID = fopen('../Latex/Thesis/epdIpSun.tex', 'w');
fprintf(FID, '\\begin{tabular}{|c|c|c|}\\hline \n');
fprintf(FID, '\\textbf{Angle of Irradiance } [deg]  & \\textbf{Relative Sensitivity} $S_{rel↩
    }$  & \\textbf{Photocurrent} $I_P$ [A]\\\\ \\hline  \n');
i=361;
for k=1:19
    fprintf(FID, '%d & %6.3f & %8.2E \\\\ ', epdSrel(i,1),epdSrel(i,2), epdIpSun(i,1));
    %if k==length(TC)
        fprintf(FID, '\\hline ');
    %end
    fprintf(FID, '\n');
    i=i+10;
end
fprintf(FID, '\\end{tabular}\n');
fclose(FID);

FID = fopen('../Latex/Thesis/epdIpAlbedo.tex', 'w');
fprintf(FID, '\\begin{tabular}{|c|c|c|}\\hline \n');
fprintf(FID, '\\textbf{Angle of Irradiance } [deg]  & \\textbf{Mean Sensitivity} $S_{mean}$ ↩
    & \\textbf{Photocurrent} $I_P$ [A]\\\\ \\hline  \n');
i=361;
for k=1:19
    fprintf(FID, '%d & %6.3f & %8.2E \\\\ ', epdSmean(i,1),epdSmean(i,2), epdIpAlbedo(i,1));
    %if k==length(TC)
        fprintf(FID, '\\hline ');
    %end
    fprintf(FID, '\n');
    i=i+10;
end
fprintf(FID, '\\end{tabular}\n');
fclose(FID);

FID = fopen('../Latex/Thesis/epdSnrSun.tex', 'w');
fprintf(FID, '\\begin{tabular}{|l|c|c|c|c|}\\hline \n');
fprintf(FID, '\\textbf{SNR} [db]    & \\textbf{25$\\degree$C}   & \\textbf{50$\\degree$C}   ↩
    & \\textbf{75$\\degree$C}   & \\textbf{100$\\degree$C}\\\\ \\hline  \n');
i=361;
for k=1:19
    fprintf(FID, '%d & %d & %d & %d & %d \\\\ ', epdSrel(i,1),epdSnrSun(i,1), epdSnrSun(i,2)↩
        , epdSnrSun(i,3), epdSnrSun(i,4));
    %if k==length(TC)
        fprintf(FID, '\\hline ');
    %end
    fprintf(FID, '\n');
    i=i+10;
end
fprintf(FID, '\\end{tabular}\n');
fclose(FID);

FID = fopen('../Latex/Thesis/epdSnrAlbedo.tex', 'w');
fprintf(FID, '\\begin{tabular}{|l|c|c|c|c|}\\hline \n');
fprintf(FID, '\\textbf{SNR} [db]    & \\textbf{25$\\degree$C}   & \\textbf{50$\\degree$C}   ↩
    & \\textbf{75$\\degree$C}   & \\textbf{100$\\degree$C}\\\\ \\hline  \n');
i=361;
for k=1:19
    fprintf(FID, '%d & %d & %d & %d & %d \\\\ ', epdSmean(i,1),epdSnrAlbedo(i,1), ↩
        epdSnrAlbedo(i,2), epdSnrAlbedo(i,3), epdSnrAlbedo(i,4));
```

```
    %if k==length(TC)
        fprintf(FID, '\\hline ');
    %end
    fprintf(FID, '\n');
    i=i+10;
end
fprintf(FID, '\\end{tabular}\n');
fclose(FID);

FID = fopen('../Latex/Thesis/epdNoise.tex', 'w');
fprintf(FID, '\\begin{tabular}{|l|c|c|c|m{3cm}|}\\hline \n');
fprintf(FID, '\\textbf{Temp} $[\\degree C]$ & \\textbf{Dark Current, $I_D$} [A] &\\textbf{↩
    Shot Current, $I_S$} [A]  &\\textbf{Thermal Noise, $I_T$}[A]  & \\textbf{Total Noise ↩
    Current, $I_{totalNoise}$} [A]\\\\ \\hline  \n');
%i=361;
for k=1:4
    fprintf(FID, '%d & %6.2E & %6.2E & %6.2E & %6.2E \\\\ ', epdId(k,1),epdId(k,2), epdIs(k↩
        ,1), epdIt(k,1), epdITotN(k,1));
    %if k==length(TC)
        fprintf(FID, '\\hline ');
    %end
    fprintf(FID, '\n');
 %   i=i+10;
end
fprintf(FID, '\\end{tabular}\n');
fclose(FID);

%BPW Sensor
FID = fopen('../Latex/Thesis/bpwIp.tex', 'w');
fprintf(FID, '\\begin{tabular}{|m{2cm}|m{2.5cm}|m{2.5cm}|m{2.5cm}|m{2.5cm}|}\\hline \n');
fprintf(FID, '\\textbf{Angle of Irradiance } [deg]  & \\textbf{Relative Sensitivity} $S_{rel↩
    }$  & \\textbf{Photocurrent} $I_{P,Sun}$ [A] & \\textbf{Mean Sensitivity} $S_{mean}$    ↩
    & \\textbf{Photocurrent} $I_{P,Albedo}$ [A] \\\\ \\hline  \n');
i=361;
for k=1:19
    fprintf(FID, '%d & %6.3f & %8.2E & %6.3f & %8.2E \\\\ ', bpwSrel(i,1),bpwSrel(i,2), ↩
        bpwIpSun(i,1), bpwSmean(i,2), bpwIpAlbedo(i,1));
    %if k==length(TC)
        fprintf(FID, '\\hline ');
    %end
    fprintf(FID, '\n');
    i=i+10;
end
fprintf(FID, '\\end{tabular}\n');
fclose(FID);

FID = fopen('../Latex/Thesis/bpwIpSun.tex', 'w');
fprintf(FID, '\\begin{tabular}{|c|c|c|}\\hline \n');
fprintf(FID, '\\textbf{Angle of Irradiance } [deg]  & \\textbf{Relative Sensitivity} $S_{rel↩
    }$  & \\textbf{Photocurrent} $I_P$ [A]\\\\ \\hline  \n');
i=361;
for k=1:19
    fprintf(FID, '%d & %6.3f & %8.2E \\\\ ', bpwSrel(i,1),bpwSrel(i,2), bpwIpSun(i,1));
    %if k==length(TC)
        fprintf(FID, '\\hline ');
    %end
    fprintf(FID, '\n');
    i=i+10;
end
fprintf(FID, '\\end{tabular}\n');
fclose(FID);

FID = fopen('../Latex/Thesis/bpwIpAlbedo.tex', 'w');
fprintf(FID, '\\begin{tabular}{|c|c|c|}\\hline \n');
fprintf(FID, '\\textbf{Angle of Irradiance } [deg]  & \\textbf{Mean Sensitivity} $S_{mean}$ ↩
    & \\textbf{Photocurrent} $I_P$ [A]\\\\ \\hline  \n');
i=361;
for k=1:19
    fprintf(FID, '%d & %6.3f & %8.2E \\\\ ', bpwSmean(i,1),bpwSmean(i,2), bpwIpAlbedo(i,1));
    %if k==length(TC)
        fprintf(FID, '\\hline ');
    %end
    fprintf(FID, '\n');
    i=i+10;
end
fprintf(FID, '\\end{tabular}\n');
fclose(FID);

FID = fopen('../Latex/Thesis/bpwSnrSun.tex', 'w');
fprintf(FID, '\\begin{tabular}{|l|c|c|c|c|}\\hline \n');
```

```
fprintf(FID, '\\textbf{SNR} [db]    & \\textbf{25$\\degree$C}   & \\textbf{50$\\degree$C}   ↩
    & \\textbf{75$\\degree$C}   & \\textbf{100$\\degree$C}\\\\ \\hline  \n');
i=361;
for k=1:19
    fprintf(FID, '%d & %d & %d & %d & %d \\\\ ', bpwSrel(i,1),bpwSnrSun(i,1), bpwSnrSun(i,2)↩
        , bpwSnrSun(i,3), bpwSnrSun(i,4));
    %if k==length(TC)
        fprintf(FID, '\\hline ');
    %end
    fprintf(FID, '\n');
    i=i+10;
end
fprintf(FID, '\\end{tabular}\n');
fclose(FID);

FID = fopen('../Latex/Thesis/bpwSnrAlbedo.tex', 'w');
fprintf(FID, '\\begin{tabular}{|l|c|c|c|c|}\\hline \n');
fprintf(FID, '\\textbf{SNR} [db]    & \\textbf{25$\\degree$C}   & \\textbf{50$\\degree$C}   ↩
    & \\textbf{75$\\degree$C}   & \\textbf{100$\\degree$C}\\\\ \\hline  \n');
i=361;
for k=1:19
    fprintf(FID, '%d & %d & %d & %d & %d \\\\ ', bpwSmean(i,1),bpwSnrAlbedo(i,1), ↩
        bpwSnrAlbedo(i,2), bpwSnrAlbedo(i,3), bpwSnrAlbedo(i,4));
    %if k==length(TC)
        fprintf(FID, '\\hline ');
    %end
    fprintf(FID, '\n');
    i=i+10;
end
fprintf(FID, '\\end{tabular}\n');
fclose(FID);

FID = fopen('../Latex/Thesis/bpwNoise.tex', 'w');
fprintf(FID, '\\begin{tabular}{|l|c|c|c|m{3cm}|}\\hline \n');
fprintf(FID, '\\textbf{Temp} $[\\degree C]$ & \\textbf{Dark Current, $I_D$} [A] &\\textbf{↩
    Shot Current, $I_S$} [A]  &\\textbf{Thermal Noise, $I_T$}[A]  & \\textbf{Total Noise ↩
    Current, $I_{totalNoise}$} [A]\\\\ \\hline  \n');
%i=361;
for k=1:4
    fprintf(FID, '%d & %6.2E & %6.2E & %6.2E & %6.2E \\\\ ', bpwId(k,1),bpwId(k,2), bpwIs(k↩
        ,1), bpwIt(k,1), bpwITotN(k,1));
    %if k==length(TC)
        fprintf(FID, '\\hline ');
    %end
    fprintf(FID, '\n');
 %   i=i+10;
end
fprintf(FID, '\\end{tabular}\n');
fclose(FID);

FID = fopen('../Latex/Thesis/tpsSnrAlbedo.tex', 'w');
fprintf(FID, '\\begin{tabular}{|p{2cm}|c|} \\hline \n');
fprintf(FID, '\\textbf{Angle of Irradiance} & \\textbf{SNR [db] at 25$\\degree$C}\\\\ \\↩
    hline  \n');

i=361;
for k=1:19
   fprintf(FID, '%d & %6.2f \\\\', VoutE(i,1),tpsSnrAlbedo(i,1));
%     fprintf(FID, '& %6.2f ', VoutE(i,1));% \\\\  \\hline \n \\textbf{SNR [dB] at 25$\\↩
    degree$C} ');
%     if k==19
        fprintf(FID, '\\hline ');
%     end
    fprintf(FID, '\n');
    i=i+10;
end
fprintf(FID, '\\end{tabular}\n');
fclose(FID);
```

A.2 Datasheets

A.2.1 EPD-365 Datasheet

Photodiode EPD-365-0-1.4

Preliminary 11.04.2007 rev. 03/07

Wavelength	Type	Technology	Case
UV	Schottky Contact	GaP	TO-46 + UG-11 filter

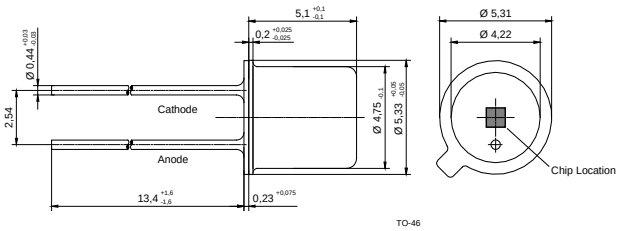

Description

Wide bandwidth and high spectral sensitivity in the UV range (245 nm - 400 nm), mounted in hermetically sealed TO-46 package with UG11 UV filter-glass window

Applications

Medical engineering (dermatology), output check of UV - lamps and gas burner flame, measurement and control of ecological parameters, radiation control for a solarium, UV water purification facilities

Miscellaneous Parameters

T_{amb} = 25℃, unless otherwise specified

Parameter	Test conditions	Symbol	Value	Unit
Active area		A	1.2	mm²
Temperature coefficient of I_D		$T_C(I_D)$	7.0	%/K
Operating temperature range		T_{amb}	-40 to +125	℃
Storage temperature range		T_{stg}	-40 to +125	℃
Acceptance angle at 50% S_λ		φ	50	deg.

Optical and Electrical Characteristics

T_{amb} = 25℃, unless otherwise specified

Parameter	Test conditions	Symbol	Min	Typ	Max	Unit
Breakdown voltage[1)]	I_R = 10 µA	V_R	5			V
Dark current	V_R = 5 V	I_D		5	30	pA
Peak sensitivity wavelength	V_R = 0 V	λ_p		365		nm
Responsivity at λ_P	V_R = 0 V	S_λ		0.07		A/W
Sensitivity range at 1%	V_R = 0 V	λ_{min}, λ_{max}	245		400	nm
Spectral bandwidth at 50%	V_R = 0 V	$\Delta\lambda_{0.5}$		85		nm
Shunt resistance	V_R = 10 mV	R_{SH}	150	200		GΩ
Noise equivalent power	λ = 365 nm	NEP		1.8×10^{-14}		$W/\sqrt{Hz}$
Specific detectivity	λ = 365 nm	D*		5.9×10^{12}		$cm \cdot \sqrt{Hz} \cdot W^{-1}$
Junction capacitance	V_R = 0 V	C_J		250		pF
Switching time (R_L = 50 Ω)	V_R = 5 V	t_r, t_f		1/20		ns
Photo current at λ = 365 nm[1,2)]	V_R = 0 V E_e = 1 mW/cm²	I_{Ph}		0.3		µA

[1)]for information only

[2)]measured with common halogen lamp source and appropriate filter

Note: All measurements carried out with *EPIGAP* equipment

Labeling

Type	Lot N°	R_D (typ.) [GΩ]	Quantity
EPD-365-0-1.4			

EPIGAP Optoelektronik GmbH, D-12555 Berlin, Köpenicker Str.325 b, Haus 201
Tel.: +49-30-6576 2543, Fax : +49-30-6576 2545

Typical responsivity

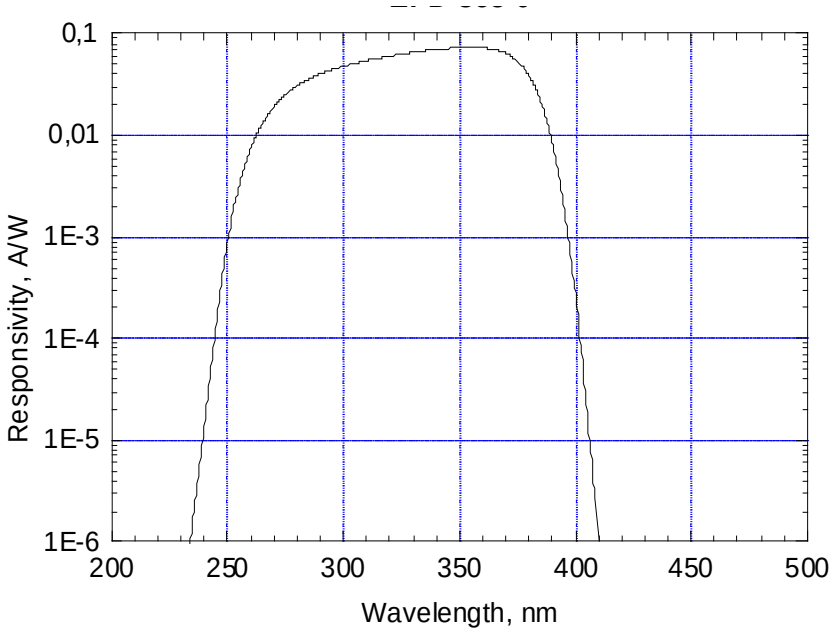

A.2.2 BPW-21 Datasheet

SIEMENS

Silizium-Fotodiode für den sichtbaren Spektralbereich — BPW 21
Silicon Photodiode for the visible spectral range

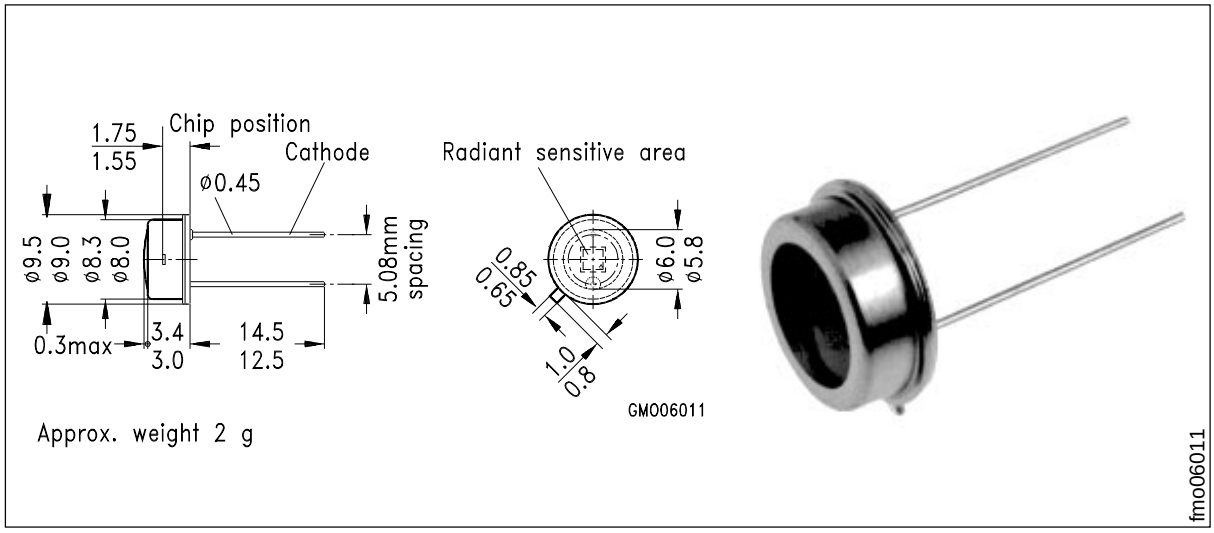

Maße in mm, wenn nicht anders angegeben/Dimensions in mm, unless otherwise specified.

Wesentliche Merkmale

- Speziell geeignet für Anwendungen im Bereich von 350 nm bis 820 nm
- Angepaßt an die Augenempfindlichkeit (V_λ)
- Hermetisch dichte Metallbauform (ähnlich TO-5), geeignet bis 125 °C[1)]

Features

- Especially suitable for applications from 350 nm to 820 nm
- Adapted to human eye sensitivity (V_λ)
- Hermetically sealed metal package (similar to TO-5), suitable up to 125 °C[1)]

Anwendungen

- Belichtungsmesser für Tageslicht
- Für Kunstlicht mit hoher Farbtemperatur in der Fotografie und Farbanalyse

Applications

- Exposure meter for daylight
- For artificial light of high color temperature in photographic fields and color analysis

Typ Type	Bestellnummer Ordering Code
BPW 21	Q62702-P885

1) Eine Abstimmung der Einsatzbedingungen mit dem Hersteller wird empfohlen bei T_A > 85 °C.

1) For operating conditions of T_A > 85 °C please contact us.

Grenzwerte
Maximum Ratings

Bezeichnung **Description**	**Symbol** **Symbol**	**Wert** **Value**	**Einheit** **Unit**
Betriebs- und Lagertemperatur Operating and storage temperature range	T_{op}; T_{stg}	– 40 ... + 80	°C
Löttemperatur (Lötstelle 2 mm vom Gehäuse entfernt bei Lötzeit $t \leq 3$ s) Soldering temperature in 2 mm distance from case bottom ($t \leq 3$ s)	T_S	235	°C
Sperrspannung Reverse voltage	V_R	10	V
Verlustleistung, T_A = 25 °C Total power dissipation	P_{tot}	250	mW

Kennwerte (T_A = 25 °C, Normlicht A, T = 2856 K)
Characteristics (T_A = 25 °C, standard light A, T = 2856 K)

Bezeichnung **Description**	**Symbol** **Symbol**	**Wert** **Value**	**Einheit** **Unit**
Fotoempfindlichkeit, V_R = 5 V Spectral sensitivity	S	10 (≥ 5.5)	nA/lx
Wellenlänge der max. Fotoempfindlichkeit Wavelength of max. sensitivity	$\lambda_{S\ max}$	550	nm
Spektraler Bereich der Fotoempfindlichkeit S = 10 % von S_{max} Spectral range of sensitivity S = 10 % of S_{max}	λ	350 ... 820	nm
Bestrahlungsempfindliche Fläche Radiant sensitive area	A	7.34	mm^2
Abmessung der bestrahlungsempfindlichen Fläche Dimensions of radiant sensitive area	$L \times B$ $L \times W$	2.73 × 2.73	mm
Abstand Chipoberfläche zu Gehäuseoberfläche Distance chip front to case surface	H	1.9 ... 2.3	mm
Halbwinkel Half angle	φ	± 55	Grad deg.

Kennwerte (T_A = 25 °C, Normlicht A, T = 2856 K)
Characteristics (T_A = 25 °C, standard light A, T = 2856 K)

Bezeichnung **Description**	**Symbol** **Symbol**	**Wert** **Value**	**Einheit** **Unit**
Dunkelstrom Dark current V_R = 5 V V_R = 10 mV	 I_R I_R	 2 (≤ 30) 8 (≤ 200)	 nA pA
Spektrale Fotoempfindlichkeit, λ = 550 nm Spectral sensitivity	S_λ	0.34	A/W
Quantenausbeute, λ = 550 nm Quantum yield	η	0.80	Electrons Photon
Leerlaufspannung, E_v = 1000 lx Open-circuit voltage	V_O	400 (≥ 320)	mV
Kurzschlußstrom, E_v = 1000 lx Short-circuit current	I_{SC}	10	µA
Anstiegs- und Abfallzeit des Fotostromes Rise and fall time of the photocurrent R_L = 1 kΩ; V_R = 5 V; λ = 550 nm; I_p = 10 µA	t_r, t_f	1.5	µs
Durchlaßspannung, I_F = 100 mA, E = 0 Forward voltage	V_F	1.2	V
Kapazität, V_R = 0 V, f = 1 MHz, E = 0 Capacitance	C_0	580	pF
Temperaturkoeffizient von V_O Temperature coefficient of V_O	TC_V	– 2.6	mV/K
Temperaturkoeffizient von I_{SC} Temperature coefficient of I_{SC}	TC_I	– 0.05	%/K
Rauschäquivalente Strahlungsleistung Noise equivalent power V_R = 5 V, λ = 550 nm	NEP	7.2×10^{-14}	$\frac{W}{\sqrt{Hz}}$
Nachweisgrenze, V_R = 5 V, λ = 550 nm Detection limit	D*	1×10^{12}	$\frac{cm \cdot \sqrt{Hz}}{W}$

Relative spectral sensitivity
$S_{rel} = f\ (\lambda)$

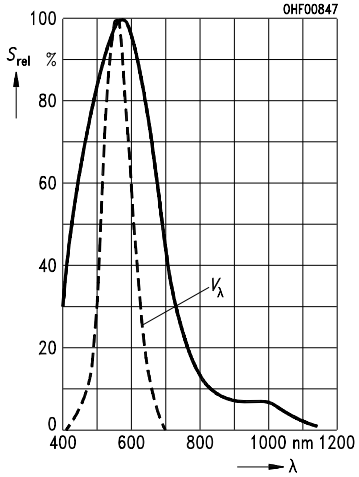

Photocurrent $I_P = f\ (E_v)$, V_R = 5 V
Open-circuit-voltage $V_O = f\ (E_v)$

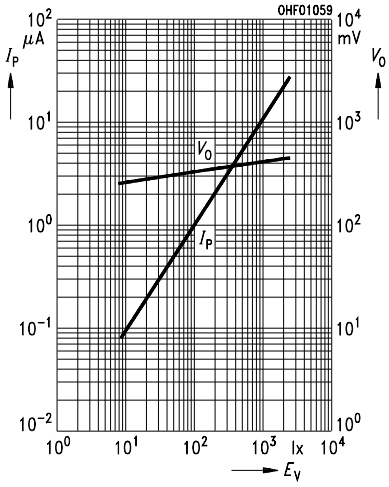

Total power dissipation
$P_{tot} = f\ (T_A)$

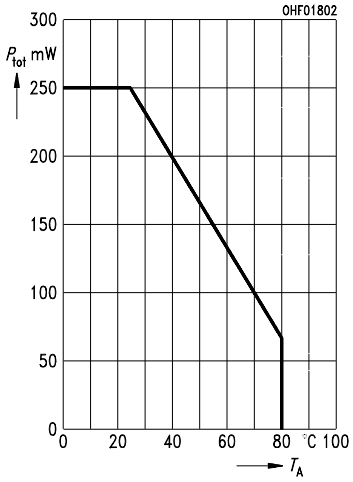

Dark current
$I_R = f\ (V_R)$

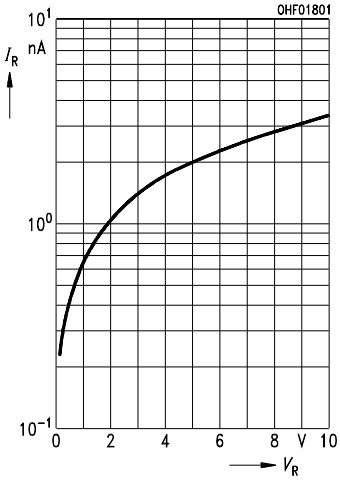

Capacitance
$C = f\ (V_R)$, f = 1 MHz, E = 0

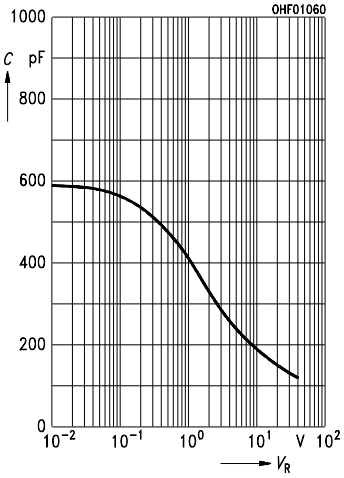

Dark current
$I_R = f\ (T_A)$, V_R = 5 V

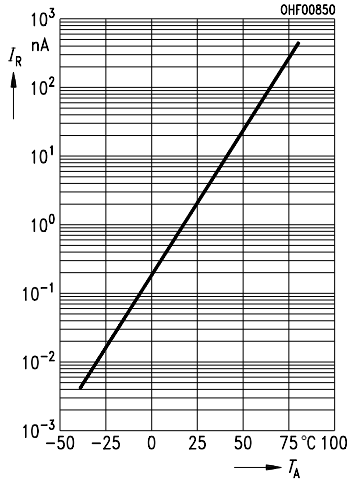

Directional characteristics $S_{rel} = f\ (\varphi)$

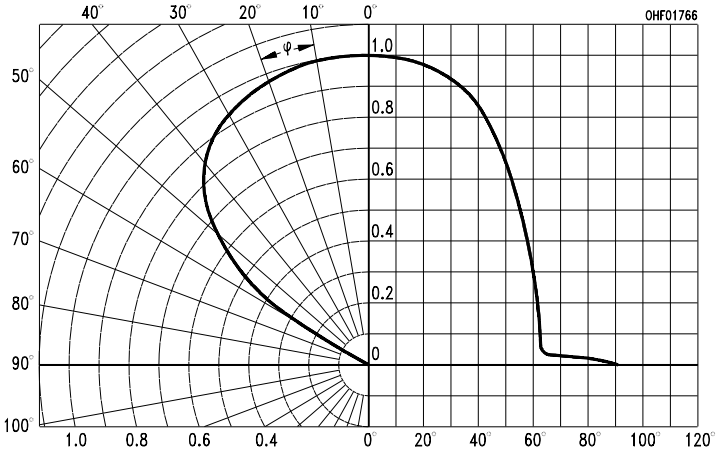

A.2.3 TPS-230 Datasheet

Thermopile Sensor

TPS 230 / 3365

Revision - Date: 2007/11/12

SENSOR SOLUTIONS

DATASHEET

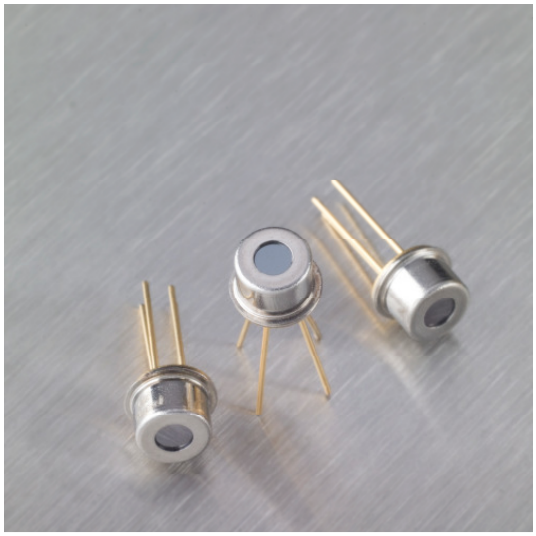

Introduction

PerkinElmer introduces the new TPS 230 as part of the TPS 23x family for low-cost remote temperature measurement applications. It consists of a silicon (Si) based thermopile chip in a metal housing with IR transmissive filter. The Si-chip carries a series of thermoelements, forming a sensitive area covered by an IR absorbing material.
With its optimized output signal, the TPS 23x family replaces the TPS 43x series by offering better performance at a lower cost.
The thermopile sensing principle allows for broadband IR measurements. PerkinElmer Opto-electronics thermopile sensors are equipped with a MEMS / MOEMS state-of-the art sensing element and an optical filter that defines the sensitive spectral range of the sensor and at the same time serves as device window.

Properties of TPS 230

The TPS 230 is a miniature thermopile sensor in the extremely small TO-41 (3.5 mm cap diameter) housing. It is especially suited for compact ear thermometer solutions. The sensor employs a very small thermopile chip with a 0.5 mm round active area allowing small spot sizes in pyrometer applications. The chip is optimized for a large output signal.
The round window is equipped with an PerkinElmer's standard IR longpass filter with 5.5 µm cut-on wavelength. The frequency behavior corresponds to a low pass characteristic.
A 100 kΩ thermistor inside the TO-housing serves as the ambient temperature reference.

Features and Benefits

- Miniature TO-41 housing (3.5 mm Ø)
- Small and perfectly round measurement spot
- Large output voltage
- High signal to noise ratio
- 5.5 µm IR longpass filter
- Stable signal in the case of ambient thermal shock due to the small TO-41 housing
- RoHS compliant – Si-chip made by standard CMOS processes

Applications

- Compact ear thermometer
- High precision remote temperature sensing
- Infrared pyrometry

PerkinElmer® precisely.

1 General Characteristics

1.1 Absolute Maximum Ratings

Table 1: Absolute Maximum Ratings

Symbol	Parameter	Min	Typ	Max	Unit	Conditions
TA	Ambient temperature range	-20		100	°C	Operation
TA	Ambient temperature range	-40		100	°C	Storage

1.2 Handling Requirements

Stresses above the absolute maximum ratings may cause damages to the device. Do not expose the sensor to aggressive detergents such as Freon, Trichloroethylene, etc. Windows may be cleaned with alcohol and cotton swab. Hand soldering and wave soldering may be applied by a maximum temperature of 260° C for a dwell time less than 10 s. Avoid heat exposure to the top and the window of the detector. Reflow soldering is not recommended.

2 Type Characteristics

2.1 Design Characteristics

The Sensor TPS 230 is a lead-free component and fully complies with the RoHS regulations.

Table 2: Design Characteristics

Parameter	Description
Cap	Metal cap with integrated IR window
Header	TO 41
Leads	(3 isolated + 1 ground) pins with solderable gold coating
Filter type	Si-based interference IR longpass filter
Temperature reference	Thermistor 100 kΩ
Insulation gas sealing	The sensor is sealed in a dry nitrogen environment and gross leak proof
Device marking	PerkinElmer Logo “P” + device number xxxx + 3 digits date code YWW

2.2 Electrical Characteristics

Table 3: Thermopile sensor characteristics

Symbol	Parameter	Min	Typ	Max	Unit	Conditions
	Sensitive Area		0.2		mm^2	Absorber Ø0.5 mm (round)
R_{TP}	Resistance	85		135	kΩ	
S_V	Responsivity		42		V/W	T_{obj} = 500 K (=227° C), T_{amb} = 298 K (=25° C) 1Hz,
ΔU / ΔT	Average sensitivity		28		µV/K	T_{obj} = 313 K (=40° C), T_{amb} = 298 K (=25° C)
ΔU / ΔT	Average sensitivity		36		µV/K	T_{obj} = 373 K (=100° C), T_{amb} = 298 K (=25° C)
τ	Time constant		15		ms	
V_{RMS}	Noise voltage		40		nV/√Hz	
	TC of resistance		0.03		%/K	
	TC of sensitivity		-0.05		%/K	

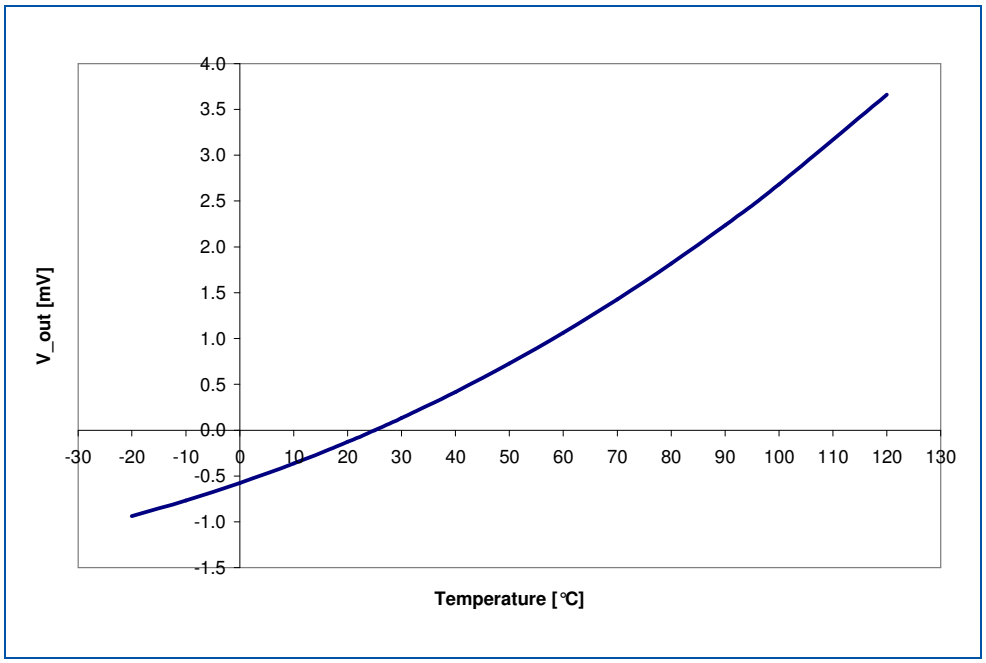

Figure 1: Typical output voltage versus object temperature with sensor at 25° C.

Table 4: Typical numerical data of Thermopile's output voltage (sensor at 25° C)

Temp.	V_out
°C	mV
-20	-0.94
-10	-0.77
0	-0.58
10	-0.36
20	-0.13
25	0.00
30	0.13
40	0.42
50	0.73
60	1.06
70	1.43
80	1.82
90	2.24
100	2.68
120	3.66

Table 5: Thermistor 100 kΩ

Symbol	Parameter	Min	Typ	Max	Unit	Conditions
R25	Base resistance	95	100	105	kΩ	Tamb = 25° C
ß	BETA -value		3964		K	Defined at 25° C/100° C
ß	BETA - tolerance			± 0.3	%	

Table 6: Tabulated Thermistor Data

Temp.	R_{min1}	R_{min2}	R_{nom}	R_{max2}	R_{max1}
°C	Ω	Ω	Ω	Ω	Ω
-20	862756	909418	915479	921581	968201
-15	655207	690548	694575	698625	733944
-10	501697	528693	531349	534018	561001
-5	387196	407985	409715	411452	432234
0	301098	317232	318336	319444	335574
5	235852	248468	249149	249832	262445
10	186038	195972	196369	196767	206701
15	147731	155608	155815	156022	163900
20	118070	124357	124439	124521	130808
25	95000	100000	100000	100000	105000
30	76707	80791	80843	80895	84978
35	62328	65649	65732	65815	69137
40	50926	53643	53743	53843	56559
45	41833	44067	44175	44283	46516
50	34541	36387	36497	36608	38453
55	28662	30195	30303	30412	31944
60	23898	25176	25280	25385	26663
65	20017	21089	21187	21286	22357
70	16842	17744	17836	17928	18830
75	14231	14994	15079	15165	15927
80	12075	12721	12800	12879	13526
85	10286	10838	10910	10983	11534
90	8796	9268	9334	9401	9872
95	7550	7956	8016	8077	8481
100	6504	6853	6908	6964	7313

R_{min1} : Minimum Thermistor Resistance resulting from the Total Tolerance
R_{min2} : Minimum Thermistor Resistance resulting from the BETA-Tolerance
R_{nom} : Typical Thermistor Resistance
R_{max1} : Maximum Thermistor Resistance resulting from the Total Tolerance
R_{max2} : Maximum Thermistor Resistance resulting from the BETA-Tolerance

2.3 Optical Characteristics

Table 7: Optical Characteristics

Symbol	Parameter	Min	Typ	Max	Unit	Conditions
	Field of view		82		degree	At 50% target signal
	Optical axis		0	+/- 10	degree	

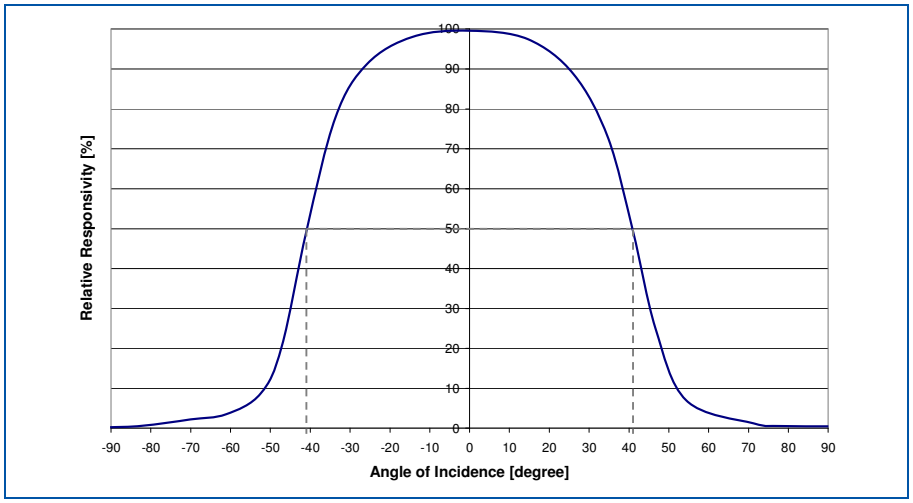

Figure 2:Field of View Curve

Table 8: Filter Parameters

Symbol	Parameter	Min	Typ	Max	Unit	Conditions
TA	Average transmittance	75	> 77		%	Wavelength range from 7.5 µm to 13.5 µm
TA	Average transmittance			< 0.5	%	Wavelength range < 5 µm
λ (5 %)	Cut on wavelength	5.2	5.5	5.8	µm	At 25°C

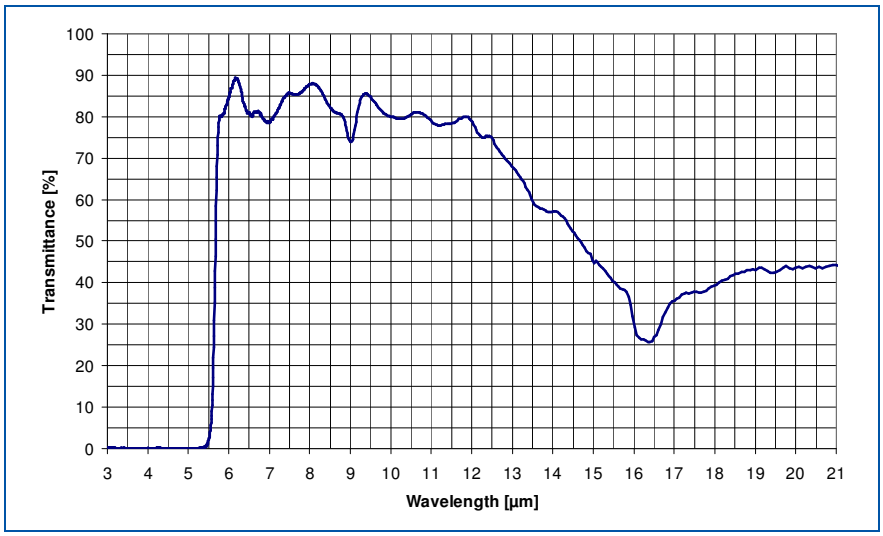

Figure 3: Transmission Curve for PerkinElmer Standard Filter

2.4 Mechanical Drawing

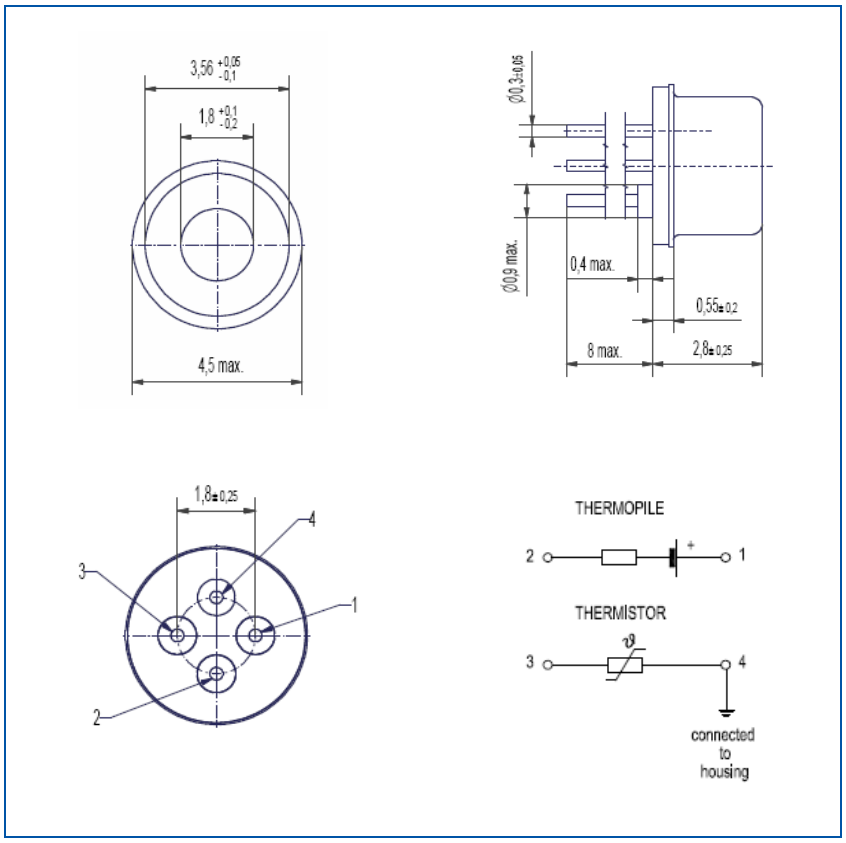

Figure 4:Mechanical Drawing of the TPS 230

3 Quality Statement

PerkinElmer Optoelectronics is an ISO 9001:2002 and ISO/TS 16949:2002 certified manufacturer. All devices employing PCB assemblies are manufactured according IPC-A-610 guidelines.

3.1 Liability Policy

The contents of this document are subject to change without notice and customers should consult with PerkinElmer Optoelectronics sales representatives before ordering. Customers considering the use of PerkinElmer Optoelectronics thermopile devices in applications where failure may cause personal injury or property damage, or where extremely high levels of reliability are demanded, are requested to discuss their concerns with PerkinElmer Optoelectronics sales representatives before such use. The Company's responsibility for damages will be limited to the repair or replacement of defective product. As with any semiconductor device, thermopile sensors or modules have a certain inherent rate of failure. To protect against injury, damage or loss from such failures, customers are advised to incorporate appropriate safety design measures into their product.

North America Customer Support Hub
PerkinElmer Optoelectronics
22001 Dumberry Road
Vaudreuil-Dorion, Québec
Canada J7V 8P7
Telephone: +1 450-424-3300, (+1) 866-574-6786 (toll-free)
Fax: +1 450-424-3345
Email: opto@perkinelmer.com
www.optoelectronics.perkinelmer.com

European Headquarters
PerkinElmer Optoelectronics
Wenzel-Jaksch-Str. 31
65199 Wiesbaden, Germany
Telephone: (+49) 611-492-247
Fax: (+49) 611-492-170
Email: opto.Europe@perkinelmer.com

Asia Headquarters
PerkinElmer Optoelectronics
47 Ayer Rajah Crescent #06-12
Singapore 139947
Telephone: (+65) 6775-2022
Fax: (+65) 6775-1008
Email: opto.Asia@perkinelmer.com

For a complete listing of our global offices, visit www.optoelectronics.perkinelmer.com

600235_01 DTS1107

A.3 CD - Contents

- ✓ Diploma Thesis Report.
- ✓ Matlab Code.
- ✓ SSBUV Data.
- ✓ Sun AM0 ASTM-E-490 Data.
- ✓ Datasheets.